Electron Paramagnetic Resonance Of Gd^{3+} In Single Crystals Of Some Hydrated Rare-Earth Nitrates And Chlorides

A thesis submitted to the Department of Physics, Indian Institute of Technology, Kanpur in partial fulfilment of the requirements for the degree of Doctor of Philosophy.

by

G.B. Singh

December, 1966

To My Uncle

20D
93

Certified that the work presented in this thesis is the original work of Mr. G.B. Singh, done under my supervision.

Putcha Venkateswarlu
Professor of Physics 30.12.66

Department of Physics
Indian Institute of Technology
Kanpur, India

Acknowledgments

This research has been carried out under the supervision of Professor Putcha Venkateswarlu, whose continuing encouragement and many valuable suggestions must be most gratefully acknowledged.

The author is thankful to Dr. P.K. Kelkar, Director, Indian Institute of Technology, Kanpur for his interest during the development of work.

Thanks are due to the Council of Scientific and Industrial Research for financial assistance in the form of a Junior Research Fellowship.

Thanks are also due to Mr. Ram Singh for fabricating crystal holder , to Graphic Arts Section for tracing and photoreproduction of figures , to the employees of Computer Section and glass blowing section for their co-operation, and to H.N. Nigam and R. Singh for their careful typing work of this thesis.

In conclusion, my appreciations to Mr. H.C. Singh, B.Tech. (Met.Engg.) for his keen interest in the Computer programming and to colleagues and friends in the EPR laboratory for their co-operation, are duly recorded.

Preface

This thesis deals with the electron paramagnetic resonance of Gd^{3+} ion in the single crystals of the following hydrated rare-earth salts at room temperature:

(a) $Pr(NO_3)_3.6H_2O$

(b) $Nd(NO_3)_3.6H_2O$

(c) $La(NO_3)_3.6H_2O$

(d) $Sm(NO_3)_3.6H_2O$

(e) $PrCl_3.7H_2O$

(f) $NdCl_3.6H_2O$

(g) $SmCl_3.6H_2O$

The four salts (a), (b), (c) and (g) are studied for the first time while a preliminary work was carried out earlier on the three remaining salts (d), (e) and (f) by Upreti of this laboratory. All the spectra corresponding to $\Delta M = \pm 1$ transitions are studied for H//Z as well as for H//X axes. Apart from the $\Delta M = \pm 1$ transitions a number of low field transitions ($\Delta M \geq 2$) are observed in the case of $Pr(NO_3)_3.6H_2O:Gd^{3+}$ and $PrCl_3.7H_2O:Gd^{3+}$. A careful study of these transitions is made for H//Z axis in both the cases. All the observed spectra are analysed in terms of the parameters of the spin Hamiltonian.

Chapter 1 is a general introduction to electron paramagentic resonanee and Chapter II deals with the theory of the rare-earth ions in crystals with emphesis on Gd^{3+}.

A paramagnetic resonance study of Gd^{3+} doped $SmCl_3.6H_2O$ is described in Chapter III and that of Gd^{3+} doped $Pr(NO_3)_3.6H_2O$ single crystals in Chapter IV.

Chapter V deals with the paramagnetic resonance of Gd^{3+} doped $NdCl_3.6H_2O$, $PrCl_3.7H_2O$, and $Sm(NO_3)_3.6H_2O$ and the Chapter VI that with the paramagnetic resonance of Gd^{3+} doped $La(NO_3)_3.6H_2O$ and $Nd(NO_3)_3.6H_2O$ single crystals. A general discussion on the zero field splittings of the ground state of Gd^{3+} in the various crystals studied here is included in Chapter VI.

The Chapters III to VI of this thesis are written in a way that they are suitable for publication. Therefore repeatition of some statements here and there in these four chapters has become unavoidable.

G.B. Singh

Department of Physics
Indian Institute of Technology, Kanpur

December 17, 1966

Contents

Preface		V
I	Introduction	1
II	General Theory of Rare Earth ions in Crystals with Emphesis on Gd^{3+}	10
III	Electron Paramagnetic Resonance of Gd^{3+} in $SmCl_3.6H_2O$ Single Crystals	22
IV	EPR Spectrum of Gadolinium in Hydrated Praseodymium Nitrate Single Crystals	31
V	EPR of Gd^{3+} doped $NdCl_3.6H_2O$, $PrCl_3.7H_2O$ and $Sm(NO_3)_3.6H_2O$ Single Crystals	40
VI	EPR Spectra of Gadolinium in Single Crystals of Hydrated Lanthanum Nitrate and Neodymium Nitrate	58

List of Figures

Fig. 1. EPR spectrum of Gd^{3+} in single crystals of $SmCl_3.6H_2O$ at H//Z direction

Fig. 2. EPR spectrum of Gd^{3+} in single crystals of $SmCl_3.6H_2O$ at H//Y direction

Fig. 3. Angular variation of the EPR of Gd^{3+} in single crystals of $SmCl_3.6H_2O$

Fig. 4. EPR spectrum of Gd^{3+} in single crystals of $Pr(NO_3)_3.6H_2O$ at H//Z direction

Fig. 5. EPR spectrum of Gd^{3+} in single crystals of $Pr(NO_3)_3.6H_2O$ at H//X direction

Fig. 6. Low field transitions of Gd^{3+} in single crystals of $Pr(NO_3)_3.6H_2O$ along with the seven $\Delta M = \pm 1$ transitions at H//Z direction

Fig. 7. EPR spectrum of Gd^{3+} in single crystals of $NdCl_3.6H_2O$ at H//Z direction

Fig. 8. EPR spectrum of Gd^{3+} in single crystals of $NdCl_3.6H_2O$ at H//X direction

Fig. 9. Angular variation of the EPR of Gd^{3+} in single crystals of $NdCl_3.6H_2O$

Fig.10. EPR spectrum of Gd^{3+} in single crystals of $PrCl_3.7H_2O$ at H//Z direction

Fig.11. EPR spectrum of Gd^{3+} in single crystals of $PrCl_3.7H_2O$ at H//X direction

Fig.12. Angular variation of the EPR of Gd^{3+} in single crystals of $PrCl_3.7H_2O$

Fig.13. Low field transitions of Gd^{3+} in single crystals of $PrCl_3.7H_2O$ along with seven $\Delta M = \pm 1$ transitions at H//Z direction

Fig.14. EPR spectrum of Gd^{3+} in single crystals of $Sm(NO_3)_3.6H_2O$ at H//Z direction

Fig.15. EPR spectrum of Gd^{3+} in single crystals of $Sm(NO_3)_3.6H_2O$ at H//X direction

Fig.16. EPR spectrum of Gd^{3+} in single crystals of $La(NO_3)_3.6H_2O$ at H//Z direction

Fig.17. EPR spectrum of Gd^{3+} in single crystals of $La(NO_3)_3.6H_2O$ at H//X direction

Fig.18. EPR spectrum of Gd^{3+} in single crystals of $Nd(NO_3)_3.6H_2O$ at H//Z direction

Fig. 19. EPR spectrum of Gd^{3+} in single crystals of $Nd(NO_3)_3.6H_2O$ at H//X direction

Fig. 20. Angular variation of the EPR of Gd^{3+} in single crystals of $La(NO_3)_3.6H_2O$.

List of Tables

1. Transformations of b_n^m.
2. Observed and calculated $\Delta M = \pm 1$ transitions of Gd^{3+} doped $SmCl_3.6H_2O$ single crystals.
3. Observed and calculated $\Delta M = \pm 1$ transitions of Gd^{3+} doped $Pr(NO_3)_3.6H_2O$ single crystals.
4. Low field transitions of Gd^{3+} doped $Pr(NO_3)_3.6H_2O$
5. The spin Hamiltonian parameters of Gd^{3+} doped $NdCl_3.6H_2O$, $PrCl_3.7H_2O$, and $Sm(NO_3)_3.6H_2O$ single crystals.
6. Observed and calculated $\Delta M = \pm 1$ transitions of Gd^{3+} doped $NdCl_3.6H_2O$, $PrCl_3.7H_2O$, and $Sm(NO_3)_3.6H_2O$ single crystals.
7. Relative separations between the zero field energy levels of Gd^{3+} in $NdCl_3.6H_2O$, $PrCl_3.7H_2O$, and $Sm(NO_3)_3.6H_2O$ single crystals.
8. Low field transitions of Gd^{3+} in $PrCl_3.7H_2O$.
9. The spin Hamiltonian parameters of Gd^{3+} doped $La(NO_3)_3.6H_2O$ and $Nd(NO_3)_3.6H_2O$ single crystals.
10. Observed and calculated $\Delta M = \pm 1$ transitions of Gd^{3+} doped $La(NO_3)_3.6H_2O$ and $Nd(NO_3)_3.6H_2O$ single crystals.
11. Relative separations between the zero field energy levels of Gd^{3+} in crystals.
12. The values of b_2^o parameter in gauss for Gd^{3+} in crystals.

Chapter I

Introduction

Electron Paramagnetic Resonance (EPR) in crystals is the process of resonant absorption of radiation by paramagnetic impurities doped in these crystals. The absorption is due to the electrons with unpaired spins in the paramagnetic ions as they undergo transitions between Zeeman energy levels. Transitions between the energy levels arising from the lowest orbital state are only absorved in the phenomenon of paramagnetic resonance, the reason being that the splitting between adjacent orbital electronic levels is of the order of 10^3 to 10^4 cm^{-1} and is much larger than the microwave frequencies used for electron paramagnetic resonance.

For the sake of simplicity let us consider a free ion with a resultant angular momentum $J = S = 1/2$. When this ion is placed in a magnetic field H, the electrons will align themselves either with their spins and moments "parallel" to the applied field, or "antiparallel" to it. The electrons will therefore now fall into two groups, and these groups will have different energies, since those with their spins aligned parallel to the field will have an energy of $1/2\ g\beta H$ less than the zero-field value and those with their spins aligned antiparallel to the field will have an energy of $1/2\ g\beta H$ greater than the zero-field value, where g is called the spectroscopic splitting factor and is a measure of the contribution of the spin and the orbital motion of the electron to its total angular momentum, and has a value of 2.0023 for a completely free spin, and $\beta = eh/4\pi mc$ is the Bohr magneton. If an alternating field of frequency ν is now applied at right angles to H, magnetic dipole

transitions are produced according to the selection rule $\Delta M = \pm 1$, where M is the quantum number of component of the angular momentum J along the field acting on the ion. The magnetic field required for a given frequency quantum is

$$h\nu = g\beta H$$

From this equation one could infer that paramagnetic resonance is observable, even at low frequencies. This, indeed, has been done by a number of workers[1]. Considerations such as the transition probabilities and the resolving power of spectrometer for observing the finer details of the spectrum, however, show that in general it is preferable to operate at the high frequencies and correspondingly high magnetic fields.

Energy will be absorbed if the spin of the electron is flipped from a direction parallel to the magnetic field to that of the anti-parallel direction. When the converse occurs, one speaks of induced emission. According to the theory of radiation, a priori probabilities of induced emission and absorption of radiation by an atomic system must be equal. For any system in thermal equilibrium there will, however, be more electrons in the ground state than in the upper state, and hence there will be a net absorption of the radiation of frequency ν .

In general, the paramagnetic ion is not free but is located on some lattice site in a crystal. In that case there are mainly two interactions; (a) interactions between the various paramagnetic ions, treated as magnetic dipoles and (b) interaction between the paramagnetic ion and the diamagnetic neighbors.

The interaction among the magnetic dipoles can be reduced

effectively to a small value by using crystals diluted with a diamagnetic isomorphous salt. Dilution of one part in a thousand of paramagnetic substance is usually sufficient to reduce this interaction to a negligible value.

Let us consider the interaction of the paramagnetic ions with the diamagnetic ligands. These ligands consist of charged ions which set up strong internal electric fields. The magnitude of the effect of this crystalline electric field will depend in large measure on the type of paramagnetic ion considered. In the representatives of the iron group, for example, the incomplete shell responsible for the paramagnetic properties of the ions is the outermost shell in the ion. The electrons in this unshielded shell are, therefore, subjected to the full effect of the crystal field. Indeed, in this case, the interaction in some ions is so strong that it results in the so called quenching of their orbital magnetic moments. In the transition group, such as the 4f-group, on the other hand, for which the incomplete shell lies more deeply embedded within the ion and is, therefore, shielded from the effects of the crystal field by a completed shell further removed from the nucleus, the situation may be quite different. The crystal field effect may then be so weak that the bound ion exhibits a spectrum very similar to that expected for the free ion.

The effect of the electric fields is to split the ground state into a number of components. The number of such components and the magnitude of the splitting depend critically on the symmetry of electric field and on its strength. The strength of the electric field, when compared with other interactions within the free ion, such as the spin-orbit or the coulomb interaction between the electrons, characterizes

the magnetic behavior of the various transition groups. In the 3d, or iron group, the crystal field is of moderate strength, being larger than the spin-orbit coupling but smaller than the coulomb interaction. In the 4d and 5d palladium and platinum groups, the crystal field is very strong and is of the same order as the coulomb interaction. In the 4f and 5f rare earth and actinide groups, the effect of the crystal field is considerably weaker than the spin-orbit coupling.

In many cases, a crystal field of high symmetry may leave the ground state degenerate. Some times, however, a combination of the spin-orbit interaction and crystal field may remove this additional degeneracy. For example Cr^{3+} has a ground state 4_F and in a cubic field of octahedral symmetry, the sevenfold orbital degeneracy is removed, into a lower singlet and two higher lying triplets. The four fold spin degeneracy is not removed even by the combined action of the cubic field and spin-orbit coupling. It is completely removed only by the addition of external magnetic field. In this case, the resulting four energy levels diverge linearly with the magnetic field and one absorption line will be observed corresponding to the superposition of the three possible $\Delta M = \pm 1$ transitions among the four levels. If a small axial field is also present, the four fold spin degeneracy is removed into two doublets. The addition of magnetic field will remove the remaining degeneracy and the levels diverge linearly with magnetic field and three absorption lines will be observed corresponding to $\Delta M = \pm 1$ transitions.

In microwave spectroscopy generally, resolution of the spectrum is limited, not by instrumental effects, but by the widths of the lines themselves. There are two major causes of line width; (a) interaction

the magnetic behavior of the various transition groups. In the 3d, or iron group, the crystal field is of moderate strength, being larger than the spin-orbit coupling but smaller than the coulomb interaction. In the 4d and 5d palladium and platinum groups, the crystal field is very strong and is of the same order as the coulomb interaction. In the 4f and 5f rare earth and actinide groups, the effect of the crystal field is considerably weaker than the spin-orbit coupling.

In many cases, a crystal field of high symmetry may leave the ground state degenerate. Some times, however, a combination of the spin-orbit interaction and crystal field may remove this additional degeneracy. For example Cr^{3+} has a ground state 4_F and in a cubic field of octahedral symmetry, the sevenfold orbital degeneracy is removed, into a lower singlet and two higher lying triplets. The four fold spin degeneracy is not removed even by the combined action of the cubic field and spin-orbit coupling. It is completely removed only by the addition of external magnetic field. In this case, the resulting four energy levels diverge linearly with the magnetic field and one absorption line will be observed corresponding to the superposition of the three possible $\Delta M = \pm 1$ transitions among the four levels. If a small axial field is also present, the four fold spin degeneracy is removed into two doublets. The addition of magnetic field will remove the remaining degeneracy and the levels diverge linearly with magnetic field and three absorption lines will be observed corresponding to $\Delta M = \pm 1$ transitions.

In microwave spectroscopy generally, resolution of the spectrum is limited, not by instrumental effects, but by the widths of the lines themselves. There are two major causes of line width; (a) interaction

between the paramagnetic ions and the lattice, and interaction between the various ions themselves. These interactions have often been treated as giving relaxation effects, characterized by two relaxation times, the spin-lattice relaxation time τ and the spin-spin relaxation time. The spin-lattice interaction determines essentially the rate at which the spin system exchanges energy with the lattice in which it is embedded. The theory of spin-lattice interactions is not well established. It has been discussed by Van Vleck[2], who considered the effect on an ion of the oscillating electric field due to the thermal vibrations of its nearest neighbors. The development of theory shows that τ is strongly temperature dependent, becoming longer as the temperature is reduced and hence reduction in line width. The theory also shows that τ depends markedly on the separation between the ground state and first excited state, if this separation is large τ is long, and if the separation is small τ is short. The broadening due to the interaction between the various paramagnetic ions, called the spin-spin interaction is independent of temperature (above the curie point) and can only be reduced by separating the magnetic carriers or by diluting the crystals with a diamagnetic isomorphous salts as mentioned earlier. Two main types of interactions between the ions have been recognized, the dipole-dipole and the exchange interactions. The dipole-dipole interaction is that due to the magnetic moments of the ions, which may be regarded like bar magnets. As with all interactions of this sort, it depends upon the angle between the spins and on the angle between the spin and the vector to the other ion.
A picture of broadening process can be obtained as follows. Each bar magnet is regarded as precessing about the external field, and can be resolved into a component which is steady and directed along the field,

together with a rotating component at right angles. The steady component sets up a steady field at any other magnet, which therefore behaves as if it is in a field which is slightly different from the external field. The rotating component sets up a rotating field, and if this rotating field has the same frequency as the frequency of precession of some other magnet there will be a couple acting on this second magnet tending to change its direction. The first process gives a broadening which is rather like that which arises from using an inhomogeneous magnetic field, and the second gives resonance broadening because it tends to reduce the life time of an ion in a given state.

The theory of the exchange interaction given by Van Vleck[3] assumes that the ions behave as free spins, and the method consists of a rigorous calculation of the area and the second and fourth moments of the absorption line. These are then used to discuss the line shapes in a qualitative way. One interesting result from Van Vleck's theory is that there is no contribution to the second moment from isotropic exchange (depends only on the relative orientation of the spins) between similar ions, but there is a contribution to the fourth moment. To make this point clear let us consider that in absence of the exchange the line shape is gaussian. When the exchange is introduced the shape will alter so that its area and second moment are unchanged while its fourth moment is increased. This suggests that the contre part of the line will be narrowed and the excess area distributed in the wings. That is, the lines will be peaked. This is the phenomenon known as exchange narrowing.

With this much of introduction to the subject of electron paramagnetic resonance, one can briefly point out a few of its applications.

(i) It provides detailed inform.tion about the variation of the ground state magnetic energy levels, and gives necessary background information for devices that make use of the ground state zeeman levels. Several practical examples include the solid-state maser amplifier and the technique of adiabatic demagnetization of paramagnetic salts at very low temperatures.

(ii) As the spectra are extremely sensitive to the symmetry and magnitude of the crystalline electric field that the paramagnetic ions experience, this technique is often used to investigate the finer details of crystal structure and bonding. Thus, information about the host lattice can be gained as a result of such studies.

(iii) When the nuclei of the paramagnetic ions themselves or, in some cases, nuclei of their immediate neighbors, have a large enough magnetic moment to cause observable hyperfine splittings, the information about the various nuclear properties can be obtained, e.g. the nuclear spin of Cr^{53} was first determined by its hyperfine structure[4].

(iv) The electron paramagnetic resonance provides experimental values for the parameters appearing in the theoretically derived spin Hamiltonian and the results can be used to provide a theoretical picture of the electronic interactions that occur in paramagnetic solids.

(v) It can be used to investigate lattice defects and phase transformations in solids.

(vi) Interesting data concerning the properties of conduction electrons in metals and semiconductors can be found.

The study that is described in the thesis has been taken up with the second of the above applications in mind.

References

1. M.A. Garstens, L.S. Singer, and A.H. Ryan, Phys. Rev. 96, 53, 1954.

2. J.H. Van Vleck, Phys. Rev., 57, 426, 1940.

3. J.H. Van Vleck, Phys. Rev., 74, 1168, 1948.

4. B. Bleaney and K.D. Bowers, Proc. Phys. Soc. (London), A64, 1135, 1951.

Books and Review Articles

1. S.A. Al'tshuler and B.M. Kozyrev, Electron Paramagnetic Resonance, (Academic Press, New York and London, 1964).

2. W. Low, Paramagnetic Resonance in Solids, (Academic Press, New York and London, 1960).

3. G.E. Pake, Paramagnetic Resonance, (W.A. Bengamin, Inc, New York, 1962).

4. D.J.E. Ingram, Free Radicals as studied by Electron Spin Resonance, (Butterworths Scientific Publications, London, 1958).

5. A. Vuylsteke, Elements of Maser Theory. (D.Van Nostrand Company, Inc., Princeton, 1962).

6. C.P. Slichter, Principles of Magnetic Resonance, (Happer and Row Publishers, New York, London, 1963).

7. B. Bleaney and K.H.W. Stevens, Repts., Progr. Phys. 16, 108, 1953.

8. K.D. Bowers and J. Owen, Ibid., 18, 304, 1955.

Chapter II

General Theory of Rare Earth ions in Crystals with Emphesis on Gd^{3+}

The Hamiltonian of the paramagnetic ion belonging to 4f cinfiguration can be written in the form

$$\mathcal{H} = H^{o} + H_{cr} + H_{z}$$

where H^{o} is the Hamiltonian of the free ion, $H_{z} = (\vec{L} + 2\vec{S})\, H_{o}$ is the energy of electrons in the external magnetic field (zeeman energy), and the energy H_{cr} is of the form

$$H_{cr} = \sum_{i} - e\, V_{c}\,(x_{i}, y_{i}, z_{i}) ,$$

where V_{c} is the potential of crystalline field, and x_{i}, y_{i}, z_{i} are the co-ordinates of the ith electron of the unfilled shell. By regarding the surrounding ions as point charges which do not overlap the paramagnetic ion, V_{c} is supposed to obey Laplace's equation, one may therefore expand V_{c} in the series of spherical harmonics

$$V_{c} = \sum_{n,m} A_{n}^{m}\; r^{n}\; Y_{n}^{m}\,(\theta, \phi)$$

When the perturbation matrix H_{cr} is calculated with the help of the wave functions of the d electrons, the spherical harmonics for which $n > 4$ will give matrix elements equal to zero, due to the orthogonality of spherical harmonics[1]. Analogously, in the case of f electrons the terms in the series with $n > 6$ can be discarded. We must also omit terms of the series with odd n, the matrix elements of odd-order spherical harmonics equal zero, since the electron wave functions are invariant under an inversion transformation. The term with $n = 0$ gives only an additional constant, which may be set equal to zero. Finally, since V_{c} is real, it follows that $A_{n}^{m} = (A_{n}^{-m})^{*}$. Further simplifications of

V_c can be obtained if one takes into account the symmetry of the crystalline field. If we denote $A_n^o r^n Y_n^o(\theta,\phi)$ by U_n^o and $[A_n^m Y_n^m(\theta,\phi) + A_n^{-m} Y_n^{-m}(\theta,\phi)]$ by $U_n^{|m|}$, the potential corresponding to the rhombic symmetry, say, will have the form

$$V_c(\text{rhombic}) = U_2^o + U_2^2 + U_4^o + U_4^2 + U_4^4 + U_6^o + U_6^2 + U_6^4 + U_6^6$$

One defines $U_n^m = B_n^m V_n^m$, where B_n^m's are related to A_n^m's through certain constant coefficients, and V_n^m's are homogeneous polynomials of degree n of coordinates x, y, z.

An ion with a total angular momentum quantum number J will have a (2J + 1) fold degeneracy in free space while this degeneracy gets lifted partially or some times completely by the effect of the crystalline field. When the number of electrons is odd the degeneracy can be lifted up to the maximum extent that one gets (J + 1) Kramer's doublets.

The matrix elements of H_{cr}, necessary for first order perturbation theory calculations, may be obtained with the help of equivalent operators. The former being connected with the corresponding equivalent operators through certain common factors, which are identical for all functions with a given n, e.g.

$$V_2^o = \alpha \bar{r^2} \left[3 J_z^2 - J(J+1)\right],$$

$$V_4^o = \beta \bar{r^4} \left[35 J_z^4 - 30 J(J+1) J_z^2 + 25 J_z^2 - 6J(J+1) + 3J^2 (J+1)^2\right], \text{ and}$$

$$V_6^o = \gamma \bar{r^6} \left[231 J_z^6 - 315 J(J+1) J_z^4 + 735 J_z^4 + 105 J^2(J+1)^2 J_z^2 - 525 J(J+1) J_z^2 + 294 J_z^2 - 5 J^3(J+1)^3 + 40 J^2 (J+1)^2 - 60 J(J+1)\right]$$

The common factors α^2, β, γ for all rare earth ions may be determined by means of the ψ functions corresponding to the states with maximum J_z.

Calculations of the splitting caused by H_{cr} in the second-order approximation requires knowledge of the matrix elements of H_{cr} connecting the ground and the first excited states:

$$\langle J+1, J_z+m \mid V_n^m \mid J, J_z \rangle \quad , \text{ where } U_n^m = B_n^m \; V_n^m$$

After the secular equation has been solved, and the energy levels of an ion in a crystalline field and the corresponding wave functions have been found, one must proceed with a calculation of the splitting of these levels by the external magnetic field and get the necessary information. With this brief introduction to the crystal field theory as applied to rare earth ions, let us come to the case of specific interest in the present study.

The ground state of Gd^{3+} is $(4f^7)\ ^8S_{7/2}$. When this ion is put in a crystal field, the ground state will remain an S state. Crystal fields can not, however, split the S state nor can the spin-orbit coupling by itself remove the eight fold degeneracy. Group theoretically considerations indicate that this degeneracy is removed even in a cubic field. Van Vleck and Penney[3] suggested that higher order perturbations involving simultaneously the crystal field and spin-orbit coupling are necessary to split the S state. The ground-state splitting is expected to be small because of the high order of perturbation. Resonance has shown that small splittings do exist, but Abragam and Pryce[4] came to the conclusion that these splittings are in fact too big to be explained by

the above process.

In a crystalline field the eight-fold degeneracy is partially removed owing to the admixture with higher states, into four two-fold levels[3,5] (Kramer's doublets). The EPR spectrum of such ion can be observed even at room temperature because of its fairly large spin-lattice relaxation time[6].

The complexity of the processes leading to a splitting of the energy levels of ion found in S state makes it difficult to undertake direct calculations. The spin-Hamiltonian method is therefore ordinarily used. When no external magnetic field exists, the spin Hamiltonian will be an even polynomial of the sixth degree in S_x, S_y and S_z, the components of spin operator along the symmetry axes x, y, and z of the local crystalline field. The number of the terms in this Hamiltonian is considerably reduced if the symmetry of the crystalline field is taken into consideration. The symmetry of the observed spectra suggests that the results can be interpretted in terms of the following spin Hamiltonian[7].

$$\mathcal{H} = g\beta \mathbf{H}.\mathbf{S} + B_2^0 O_2^0 + B_2^2 O_2^2 + B_4^0 O_4^0 + B_4^2 O_4^2 + B_4^4 O_4^4 + B_6^0 O_6^0 + B_6^2 O_6^2 + B_6^4 O_6^4 + B_6^6 O_6^6$$

with $S = 7/2$. (1)

The first term gives the interaction with the applied external magnetic field and the remaining terms relate to the splittings of the electronic levels in zero magnetic field. The operators O_n^m are homogeneous functions of degree n of the angular momentum operators S_z, S_+, and S_-, called the operator equivalents[8]. They transform like

the symmetry operations of the point symmetry of the site of the rare earth ion and B_n^m are coefficients dependent upon the crystal field and are to be determined by the experiment. The explicit form of the operators O_n^m is as follows:

$$O_2^0 = \left[3 S_z^2 - S(S+1)\right] ,$$

$$O_2^2 = \tfrac{1}{2} \left(S_+^2 + S_-^2 \right),$$

$$O_4^0 = \left[35 S_z^4 - \left\{30 S(S+1) - 25\right\} S_z^2 - 6 S(S+1) + 3S^2(S+1)^2\right],$$

$$O_4^2 = \tfrac{1}{4} \left[\left\{7 S_z^2 - S(S+1) - 5\right\} \left(S_+^2 + S_-^2\right) + \left(S_+^2 + S_-^2\right)\left\{7S_z^2 - S(S+1) - 5\right\}\right] ,$$

$$O_4^4 = \tfrac{1}{2} \left(S_+^4 + S_-^4\right)$$

$$O_6^0 = \left[231 S_z^6 - 315 S(S+1) S_z^4 + 735 S_z^4 + 105 S^2 (S+1)^2 S_z^2 - 525 S(S+1) S_z^2 + 294 S_z^2 - 5 S^3 (S+1)^3 + 40 S^2 (S+1)^2 - 60 S(S+1)\right] .$$

$$O_6^2 = \tfrac{1}{4} \left[\left\{33 S_z^4 - 18 S(S+1) S_z^2 - 123 S_z^2 + S^2(S+1)^2 + 10S (S+1) + 102\right\} \left(S_+^2 + S_-^2\right) + \left(S_+^2 + S_-^2\right) \left\{33S_z^4 - 18S(S+1) S_z^2 - 123 S_z^2 + S^2(S+1)^2 + 10S(S+1) + 102\right\}\right] ,$$

$$O_6^4 = \tfrac{1}{4} \left[\left\{11 S_z^2 - S(S+1) - 38\right\} \left(S_+^4 + S_-^4\right) + \left(S_+^4 + S_-^4\right) \left\{11 S_z^2 - S(S+1) - 38\right\}\right] ,$$

$$O_6^6 = \tfrac{1}{2} \left(S_+^6 + S_-^6\right) \qquad (2)$$

where $S_{\pm} = S_x \pm S_y$

It is convenient to make the following substitutions[9]:

$$b_2^0 = 3\,B_2^0,\quad b_4^0 = 60\,B_4^0,\quad b_6^0 = 1260\,B_6^0,$$

$$b_2^2 = 3B_2^2,\quad b_4^2 = 60\,B_4^2,\quad b_4^4 = 60\,B_4^4,$$

$$b_6^2 = 1260\,b_6^2,\quad b_6^4 = 1260\,b_6^4,\quad b_6^6 = 1260\,B_6^6. \qquad (3)$$

The present calculation takes into account the second order perturbation by b_2^2 and neglects the corrections due to other off-diagonal terms. For H//Z the spin Hamiltonian (1) takes the following form

$$\mathcal{H} = \beta\, g_{\parallel} H_z S_z + \tfrac{1}{3} b_2^0 O_2^0 + 1/60\, b_4^0 O_4^0 + 1/1260\, b_6^0 O_6^0 + \tfrac{1}{3} b_2^2 O_2^2 \qquad (4)$$

The expressions for the energy levels for H//Z upto second order in b_2^2 by making use of the matrix elements[7] of O_2^0, O_2^2, O_4^0, and O_6^0 between the various states characterized by J_z's within J, are given as follows

$$E_{\pm 7/2} = \pm 7/2\, g\beta H + 7 b_2^0 + 7 b_4^0 + b_6^0 + (b_2^2)^2/18 \left[21/\pm g\beta H + 5b_2^0\right],$$

$$E_{\pm 5/2} = \pm 5/2\, g\beta H + b_2^0 - 13b_4^0 - 5b_6^0 + (b_2^2)^2/18 \left[45/\pm g\beta H + 3b_2^0\right],$$

$$E_{\pm 3/2} = \pm 3/2\, g\beta H - 3b_2^0 - 3b_4^0 + 9b_6^0 + (b_2^2)^2/18 \left[(60/\pm g\beta H + b_2^0) + (21/\pm g\beta H - 5b_2^0)\right],$$

$$E_{\pm 1/2} = \pm \tfrac{1}{2} g\beta H - 5b_2^0 + 9b_4^0 - 5b_6^0 + (b_2^2)^2/18 \left[(60/\pm g\beta H - b_2^0) + (45/\pm g\beta H - 3b_2^0)\right]. \qquad (5)$$

The resonance field equations for H//Z corresponding to $\Delta M = \pm 1$ transitions, using (5) will be given by

$$\pm 7/2 \leftarrow \pm 5/2 \quad : \quad g\beta H = h\nu \mp (6\, b_2^0 + 20\, b_4^0 + 6\, b_6^0) + E\left[(45/1 \pm 3F) - (21/1 \pm 5F)\right] ,$$

$$\pm 5/2 \rightarrow \pm 3/2 \quad : \quad g\beta H = h\nu \mp (4b_2^0 - 10b_4^0 - 14b_6^0) + E\left[(60/1 \pm F) - (21/1 \pm 5F) - (45/1 \pm 3F)\right] ,$$

$$\pm 3/2 \rightarrow \pm 1/2 \quad : \quad g\beta H = h\nu \mp (2\, b_2^0 - 12b_4^0 + 14b_6^0) + E\left[(21/1 \pm 5F) - (45/1 \pm 3F) - (120F/1 - F^2)\right] ,$$

$$1/2 \rightarrow -1/2 \quad : \quad g\beta H = h\nu + E\left[(90/1 - 9F^2) - (120/1 - F^2)\right] , \qquad (6)$$

where $F = b_2^0/g\beta H$; $E = (b_2^2)^2 / 18\, g\beta H$, ν is the frequency of the microwave radiation, and h is Planck's constant.

The resonance field equations for H//X corresponding to $\Delta M = \pm 1$ transitions can be obtained from (6) by applying the transformations[7] of b_n^m, given in table 1.

Table 1

Transformations of b_n^m .

z-axis	x-axis
b_2^0	$1/2\ (-b_2^0 + b_2^2)$
b_4^0	$1/8\ (3b_4^0 - b_4^2 + b_4^4)$
b_6^0	$1/16\ (-5b_6^0 + b_6^2 - b_6^4 + b_6^6)$
b_2^2	$1/2\ (-3b_2^0 - b_2^2)$

The magnitudes as well as the relative signs of the diagonal terms b_2^0, b_4^0, and b_6^0, which are dominant when H//Z, are found to a first approximation by neglecting the off-diagonal terms proportional to E. The parameter b_2^2 can be determined by measuring the spectrum in H//X direction. The value of b_2^2 is then inserted in equ. (6) and the values of the diagonal terms are re-evaluated and the process is repeated to get consistent values of b's.

By making use of (5) it can be shown that the resonance field equations for H//Z corresponding to the low field transitions ($\Delta M \geq 2$) are as follows:

$$\pm 7/2 \leftrightarrow \pm 3/2 \;:\; g\beta H = 1/2\Big[\, h\nu \mp (10b_2^0 \mp 10b_4^0 \pm 8b_6^0) + E\Big[(60/1 \pm F) - (42/1 \pm 5F)\Big] \;,$$

$$\pm 5/2 \leftrightarrow \pm 1/2 \;:\; g\beta H = 1/2\Big[\, h\nu \mp (6b_2^0 \pm 22b_4^0) + E\Big[(60/1 \mp F) - (90/1 \pm 3F)\Big] \;,$$

$$\pm 3/2 \leftrightarrow \mp 1/2 \;:\; g\beta H = 1/2\Big[\, h\nu \mp (2b_2^0 \pm 12b_4^0 \mp 14b_6^0) + E\Big[(45/1 \mp F) + (21/1 \pm 5F) - (120/1 \pm F)\Big] \;,$$

$$\pm 7/2 \leftrightarrow \pm 1/2 \;:\; g\beta H = 1/3\Big[h\nu \mp (12b_2^0 \pm 2b_4^0 \mp 6b_6^0) + E\Big[(60/1 \mp F) - (45/1 \pm 3F) - (21/1 \pm 5F)\Big] \;,$$

$$\pm 5/2 \leftrightarrow \mp 1/2 \;:\; g\beta H = 1/3\Big[h\nu - (6b_2^0 + 22b_4^0) + E\Big[(45/1 \mp 3F) - (60/1 \pm F) - (45/1 \pm 3F)\Big] \;,$$

$$3/2 \rightarrow -3/2 \;:\; g\beta H = 1/3\Big[h\nu + E\Big[(42/1 - 25F^2) - (120/1 - F^2)\Big]$$

$$\pm 7/2 \leftrightarrow \mp 1/2 \;:\; g\beta H = 1/4\left[h\nu \mp (12b_2^0 \pm 2b_4^0 - 6b_6^0) + E\left\{(45/1-3F) - (60/1+F) - (21/1+5F)\right\}\right] ,$$

$$\pm 5/2 \leftrightarrow \mp 3/2 \;:\; g\beta H = 1/4\left[h\nu \mp (4b_2^0 \pm 10b_4^0 \pm 14b_6^0) + E\left\{(21/1\mp 5F) - (60/1\mp F) - (45/1 \pm 3F)\right\}\right] ,$$

$$\pm 7/2 \leftrightarrow \mp 3/2 \;:\; g\beta H = 1/5\left[h\nu \mp (10b_2^0 \mp 10b_4^0 \pm 8b_6^0) + E\left\{(\pm 210F/1-25F^2) - (60/1 \mp F)\right\}\right] ,$$

$$5/2 \rightarrow -5/2 \;:\; g\beta H = 1/5\left[h\nu - E\,(90/1-9F^2)\right] ,$$

$$\pm 7/2 \leftrightarrow \mp 5/2 \;:\; g\beta H = 1/6\left[h\nu \mp (6b_2^0 \mp 20b_4^0 \mp 6b_6^0) - E\left\{(21/1 \pm 5F) + (45/1 \mp 3F)\right\}\right] ,$$

$$7/2 \rightarrow -7/2 \;:\; g\beta H = 1/7\left[h\nu - E\,(42/1 - 25F^2)\right] . \qquad (7)$$

The zero-field energy levels can be found by diagonalizing the 8x8 matrix given on page 20 with H = 0 and substituting the values of b parameters obtained from the spin Hamiltonian analyses.

Signs of the constants

The absolute sign of b_2^0 is usually found by observing the relative intensities[10] of the lines at $\theta = 0^\circ$ at low temperatures (4.2°K). According to equation (6), b_2^0 will be positive if the intensity of the high field lines at low temperatures is greater than that of the low field lines, and b_2^0 will be negative if the intensity of the low field lines is greater than that of the high field lines. The absolute sign of b_2^0 could not be determined in the present experiments as the

measurements made here are at room temperature and as the work at liquid helium temperature is not yet started in this laboratory. Therefore b_2^o is assumed to be positive and the relative signs of the different b parameters are found.

	7/2	5/2	3/2	1/2	-1/2	-3/2	-5/2	-7/2
7/2	$3.5H + {}^{7}b_2^o + {}^{7}b_4^o + {}^{7}b_6^o$	0	$\sqrt{7/3}\ {}^{2}b_2$	0	0	0	0	0
5/2	0	$2.5H+{}^{5}b_2^o-13{}^{5}b_4^o-5{}^{5}b_6^o$	0	$\sqrt{5}\ {}^{2}b_2$	0	0	0	0
3/2	$\sqrt{7/3}\ {}^{2}b_2$	0	$1.5H-3{}^{3}b_2^o-3{}^{3}b_4^o+9{}^{3}b_6^o$	0	$2/3\sqrt{15}\ {}^{2}b_2$	0	0	0
1/2	0	$\sqrt{5}\ {}^{2}b_2$	0	$.5H-5{}^{1}b_2^o+9{}^{1}b_4^o-5{}^{1}b_6^o$	0	$2/3\sqrt{15}\ {}^{2}b_2$	0	0
-1/2	0	(	$2/3\sqrt{15}\ {}^{2}b_2$	0	$-.5H-5{}^{-1}b_2^o+9{}^{-1}b_4^o-5{}^{-1}b_6^o$	0	$\sqrt{5}\ {}^{2}b_2$	0
-3/2	0	0	0	$2/3\sqrt{15}\ {}^{2}b_2$	0	$-1.5H-3{}^{-3}b_2^o-3{}^{-3}b_4^o+9{}^{-3}b_6^o$	0	$\sqrt{7/3}\ {}^{2}b_2$
-5/2	0	0	0	$\sqrt{5}\ {}^{2}b_2$	0	0	$-2.5H+{}^{-5}b_2^o-13{}^{-5}b_4^o-5{}^{-5}b_6^o$	0
-7/2	0	0	0	0	$\sqrt{7/3}\ {}^{2}b_2$	0	0	$-3.5H+{}^{-7}b_2^o+{}^{-7}b_4^o+{}^{-7}b_6^o$

References

1. L. Landau, Ye Lifshits, Quantum Mechanics, Gostekhiz dat, 1948.
2. K.W.H. Stevens, Proc. Phys. Soc, A65, 209, 1952.
3. J.H. Van Vleck and W.G. Penney, Phil. Mag.(7) 17, 961, 1934.
4. G. Feher, H.E.D. Scovil, Phys. Rev. 105, 760, 1957.
5. A. Abragam, and M.H.L. Pryce, Proc. Roy. Soc. A205, 135, 1951.
6. R. Lacroix, Helv. Phys. Acta, 30, 374, 1957.
7. D.A. Jones, J.M. Baker and D.F. Pope, Proc. Phys. Soc. 74, 249, 1959.
8. J.M. Baker, B. Bleaney, and W. Hayes, Proc. Roy. Soc.(London) A 247, 141, 1958.
9. C.F. Hemstead and K.D. Bowers, Bell Telephone System Technical Publications monograph 3599.
10. B. Bleaney, H.E.D. Scovil, and R.S. Trenam, Proc. Roy. Soc. (London) A 223, 15, 1954.
11 Proc. Phys. Soc. London A 219 [illegible]

Chapter III

Paramagnetic Resonance* of Gd^{3+} in $SmCl_3.6H_2O$ Single Crystals

Abstract

The paramagnetic resonance of Gd^{3+} in $SmCl_3.6H_2O$ single crystals, is studied at room temperature. A six line spectrum for H//Z and a seven line spectrum for H//X corresponding to $\Delta M = \pm 1$ transitions are observed. Their angular variation in ZX plane from $\theta = 0^\circ$ to $\theta = 90^\circ$, is studied and the spin Hamiltonian analysis is presented. The probable amount of admixture of the next higher electronic state $^6P_{7/2}$ with the ground state $^8S_{7/2}$ is also estimated.

---

* To be published in the Proc. Ind. Acad. Sc.

Introduction

It was felt that it would be interesting to study the EPR of Gd^{3+} in salts like $SmCl_3.6H_2O$ as such salts, though paramagnetic in nature, can serve as good diamagnetic hosts, because of the short spin-lattice relaxation time of the paramagnetic ion of the salts. Earlier Bogle, and Heine[1] have reported the results on $Gd_2(SO_4)_3.8H_2O$, Garif'yanov[2] on $Gd(NO_3)_3.6H_2O$, Weger and Low[3] on Gd^{3+} doped $LaCl_3.7H_2O$, and Johnston, Wong, and Stafsudd[4] on Gd^{3+} doped $La_2(SO_4)_3.9H_2O$ single crystals. The present chapter deals with the paramagnetic resonance of Gd^{3+} doped $SmCl_3.6H_2O$ single crystals.

Experimental Details and Sample Preparation

A Varian V-4502 X-band EPR spectrometer with 100kc field modulation is used along with a rotable 9-inch magnet. The sample is placed in cylindrical cavity along with a minute sample of Diphenyl picryal hydrazil which is used as a standard for calibration, its g value being 2.0036. The magnetic field is measured with the help of a Varian F-8 Fluxmeter and the frequency is counted with a Hewlett packard counter 524-C. All the calculations are done using an IBM 1620 computer.

$SmCl_3.6H_2O$ is a monoclinic crystal[5] with $\beta = 93^{\circ}\ 40'$, $a = 9.6\text{Å}$, $b = 6.61\text{Å}$, and $c = 8.0\text{Å}$. The crystallographic structure is not available. Single crystals are grown by slow evaporation of the solution of $SmCl_3.6H_2O$ having a small amount of gadolinium as impurity to which about 0.05 mole percent of the latter has been further added.

Experimental Results

The resonance field equations for H//Z corresponding to $\Delta M = \pm 1$ transitions are given in chapter II along with the transformations of b_n^m needed to get the resonance field equations for H//X. The observed spectra for H//Z and H//X are shown in figs. 1, and 2, respectively. The peak to peak derivative width of the absorption lines is about 60-150 gauss. The angular variation of the observed spectrum in ZX plane from $\theta = 0^\circ$ to $\theta = 90^\circ$, is shown in fig. 3, that in the range $\theta = 90^\circ - 180^\circ$ being a mirror image of this. The zero-field splittings of the levels is such that while one observes seven lines for H//X, only six lines are observed for H//Z. In fact all the seven lines can be followed from $\theta = 90^\circ$ to $\theta = 48^\circ$, the seventh line being unobservable for $\theta < 48^\circ$ where θ is the angle between H and Z-axis. The absorpition lines other than $\Delta M = \pm 1$ transitions for H//Z and H//X might be corresponding to the low field transitions ($\Delta M \geq 2$).

The parameters of the spin Hamiltonian have been obtained in the manner described in the chapter II and are as given below;

$g_{\parallel} = 1.990 \pm .002$, $g_{\perp} = 1.990 \pm .002$, $b_2^0 = 667.7$ gauss,

$b_4^0 = -12.0$ gauss, $b_6^0 = -0.87$ gauss, $b_2^2 = -426.3$ gauss,

$b_4^4 - b_4^2 = 48.64$ gauss, and $b_6^6 - b_6^4 + b_6^2 = -11.39$ gauss.

The calculated resonance fields for H//Z corresponding to $\Delta M = \pm 1$ transitions using the above parameters are given in table 2 along with the observed resonance fields for H//Z as well as for H//X.

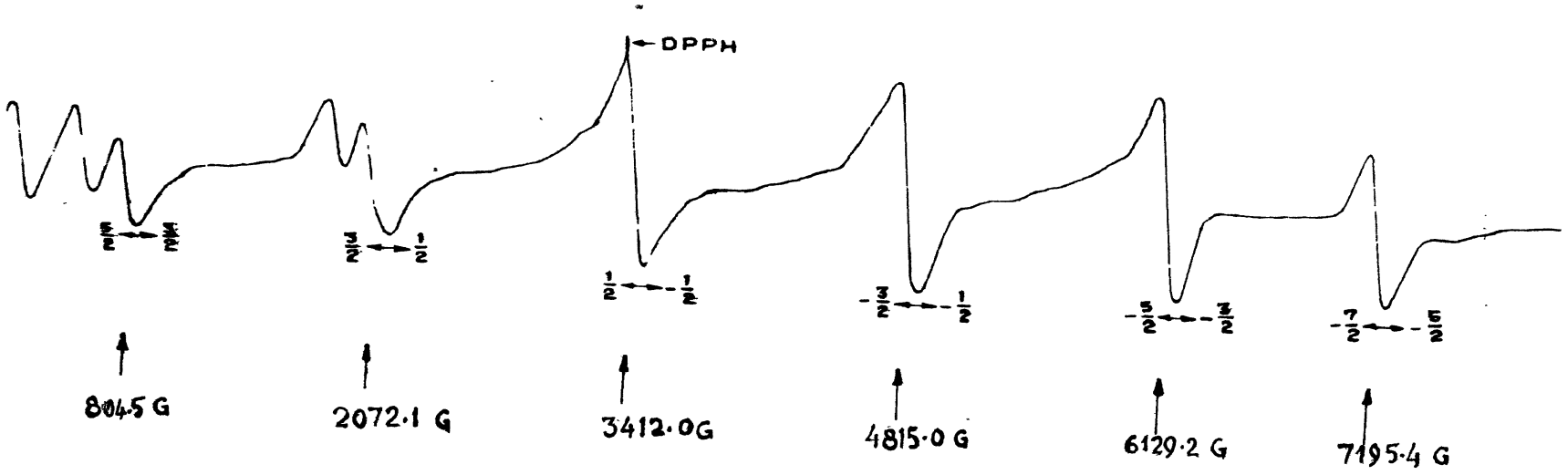

Fig. 1. EPR spectrum of Gd^{3+} in single crystals of $SmCl_3 . 6H_2O$ at H//Z direction

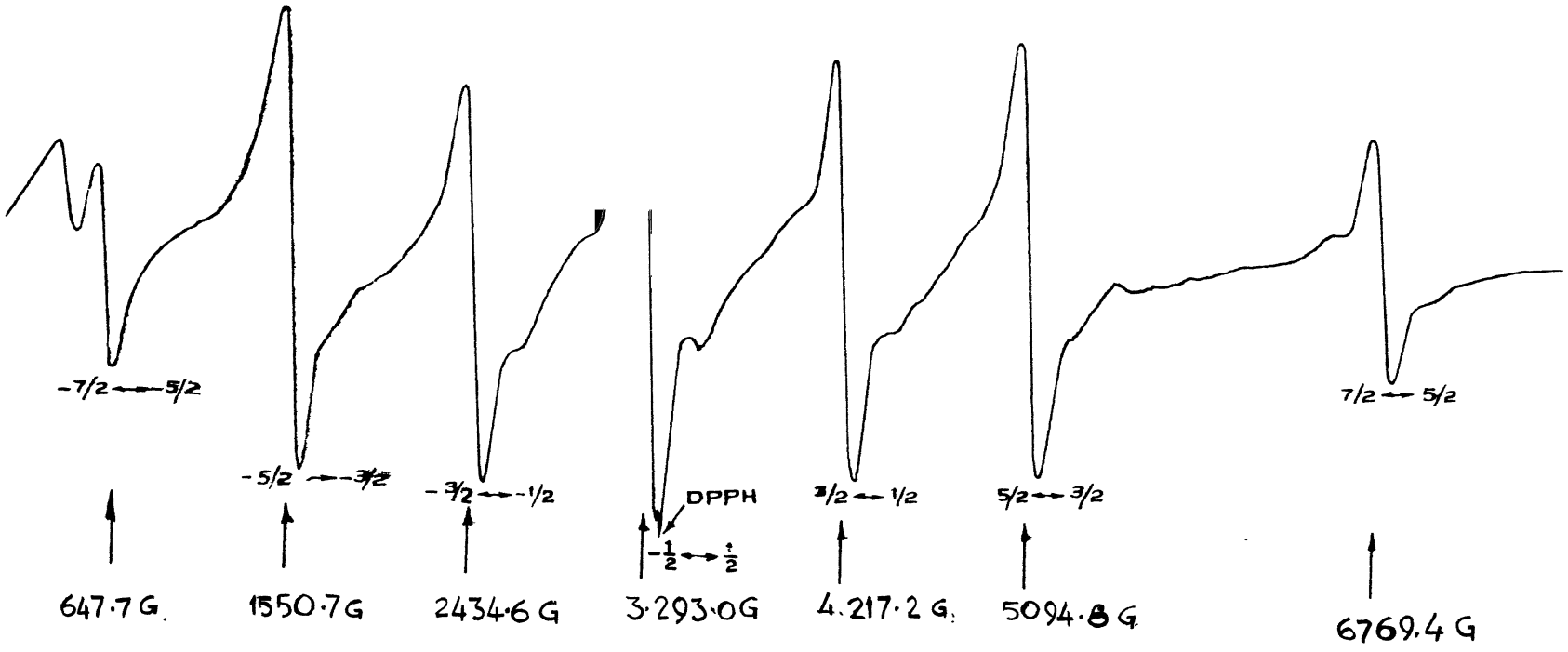

Fig. 2. EPR spectrum of Gd^{3+} in single crystals of $SmCl_3.6H_2O$ at H//X direction

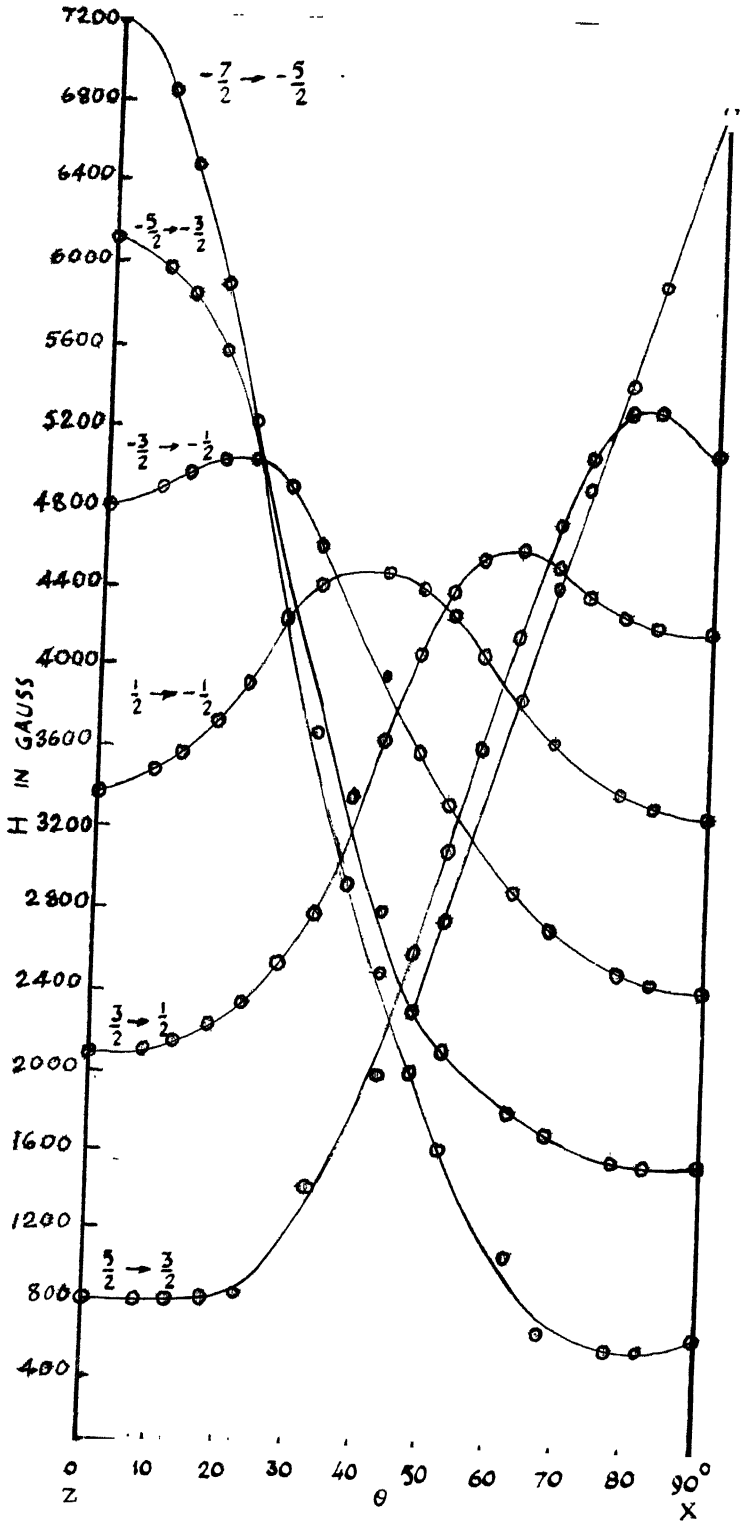

Fig. 3. Angular variation of the EPR of Gd^{3+} in single crystals of $SmCl_3.6H_2O$

Table 2

Observed and Calculated $\Delta M = \pm 1$ transitions of Gd^{3+} doped $SmCl_3.6H_2O$ single crystals

Transition	H paralle to the Z-axis observed*	Calculated	H paralle to the X-axis observed*
5/2 → 7/2	not observable		6769.4 (G)
3/2 → 5/2	804.5 (G)	794.0 (G)	5094.8
1/2 → 3/2	2072.1	2072.7	4217.2
-1/2 → 1/2	3412.0	3417.1	3293.0
-3/2 → -1/2	4815.0	4815.7	2434.6
-5/2 → -3/2	6129.2	6129.8	1550.7
-7/2 → -5/2	7195.4	7195.5	647.7
DPPH marker		3352.4 (G)	

* Error involved in the observed field values is around ±5 G.

The relative separations between the four doublets corresponding to zero-field energy levels, are found to be approximately 10 kmc ($\pm 7/2 \leftrightarrow \pm 5/2$), 7.1 kmc ($\pm 5/2 \leftrightarrow \pm 3/2$), and 7.4 kmc ($\pm 3/2 \leftrightarrow \pm 1/2$), respectively.

Discussions

The $+ 7/2 \rightarrow + 5/2$ transition could not be observed for H//Z as the zero-field splittings of ($\pm 7/2 \leftrightarrow \pm 5/2$) is about 10 kmc which is larger than the maximum frequency of the spectrometer used. One may expect to observe this transition and therefore all the seven transitions of the Gd^{3+} ion by doing the EPR work in the K-band region or other higher

frequency regions.

The g-value observed in the present work is 1.990 $\pm$ .002 which is less than that of the free electron value. Such deviation in g-value in the case of Gd^{3+} has been observed by earlier workers and was explained probably due to an admixture of the next higher electronic state $^6P_{7/2}$ with the ground state $^8S_{7/2}$. Assuming this to be the reason, the admixture parameter α is estimated to be about 0.20 using the following formula indicated by earlier workers[6],

$$g = (1 - \alpha^2)\, g_S + \alpha^2\, g_P$$

where $g_S = 2.0023$, and $g_P = 1.716$, are the g-values for $^8S_{7/2}$ and $^6P_{7/2}$ states, respectively.

References

1. G.S. Bogle, and V. Heine, Proc. Phys. Soc. A67, 734, 1954.

2. N.S. Garif'yanov, Dokl. Akad. Nauk SSSR, 84, No.5, 923, 1952.

3. M. Weger and W. Low, Phys. Rev. 111, 1526, 1958.

4. D.R. Johnston E.Y. Wong, and O.M. Stofsudd, J.Chem. Phys. 44, 2693, 1966.

5. ACA monograph number 5- crystal data determinative tables (2nd addition) Donnay and Donnay.

6. R. Lacroix, Helv. Phys. Acta, 30, 374, 1957.

Chapter IV

Paramagnetic Resonance* of Gd^{3+} doped $Pr(NO_3)_3.6H_2O$ single crystals

Abstract

The paramagnetic resonace spectrum of Gd^{3+} doped $Pr(NO_3)_3.6H_2O$ single crystals, is studied at room temperature. A seven line spectrum for H//Z as well as for H//X corresponding to $\Delta M = \pm 1$ transitions is observed along with a number of low field transitions ($\Delta M \geq 2$). The spin Hamiltonian analysis is presented.

---

* communicated to the Proc. Ind. Acad. Sc.

Introduction

A paramagnetic resonance study of Gd^{3+} doped $SmCl_3.6H_2O$ single crystals is described by the author in Chapter III. The present Chapter deals with the paramagnetic resonance of Gd^{3+} doped $Pr(NO_3)_3.6H_2O$ single crystals.

Experimental Results

The resonance field equations used here are the same as given in Ch. II .The experimental procedure and the method of growing Gd^{3+} doped $Pr(NO_3)_3.6H_2O$ single crystals are the same as given in Chapter III. $Pr(NO_3)_3.6H_2O$ is a triclinic crystal for which no crystallographic structure seems to be available. The EPR of Gd^{3+} doped in this crystal shows a seven line spectrum for H//Z as well as for H//X corresponding to $\Delta M = \pm 1$ transitions. The spectra obtained are given in figs. 4, and 5, respectively. The peak to peak derivative width of $\Delta M = \pm 1$ transitions is about 14 - 17 gauss. Apart from the $\Delta M = \pm 1$ transitions a number of low field transitions are observed. These varied in position and intensity as the magnetic field is rotated with respect to the Z-axis. A careful study of these lines is made for H//Z direction and the observed transitions are shown in fig. 6, along with $\Delta M = \pm 1$ transitions. The parameters of the spin Hamiltonian have been obtained in the manner described in Chapter II and are as given below:

$$g_{\parallel} = 1.993 \pm .002 \ , \ g_{\perp} = 1.987 \pm .002, \ b_2^0 = 488.5 \text{ gauss},$$

b_4^0 = 1.6 gauss , b_6^0 = 0.11 gauss, b_2^2 = -377.5 gauss, $b_4^4 - b_4^2$ = 11.2 gauss, and $b_6^6 - b_6^4 + b_6^2$ = 5.83 gauss.

The resonance fields corresponding to $\Delta M = \pm 1$ transitions for H//Z, calculated using the parameters given above, are given in table 3 along with the observed resonance fields for H//Z. The corresponding observed values for H//X are also included in table 3. The relative separations between the four doublets corresponding to zero-field energy levels, are found to be approximately 7.74 kmc ($\pm 7/2 \leftrightarrow \pm 5/2$), 4.93 kmc ($\pm 5/2 \leftrightarrow \pm 3/2$), and 6.01 kmc ($\pm 3/2 \leftrightarrow \pm 1/2$), respectively.

It may be noted here that Drumheller[1] has reported earlier low field transitions upto $\Delta M = \pm 4$ in the case of $BaF_2 : Gd^{3+}$ and Low and Shaltiel[2] reported transitions upto $\Delta M = \pm 5$ in the case of $ThO_2 : Gd^{3+}$. An attempt is made to identify the low field transitions in the present experiments by comparing the observed transitions with the theoretically expected positions. The resonance fields corresponding to these lines are listed in table 4 along with the assigned transitions and theoretically expected resonance fields. The assignments are to be taken as tentative as these are involving very large values of ΔM. These assignments, if correct, indicate the presence of a large amount of mixing of the different states at low field values.

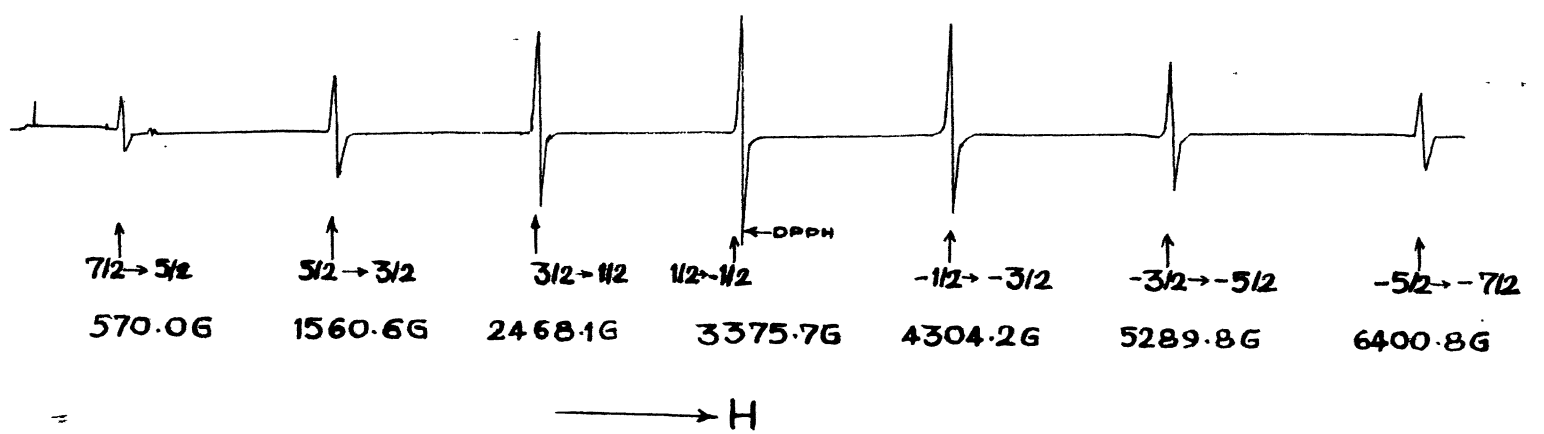

Fig. 4. EPR spectrum of Gd^{3+} in single crystals of $Pr(NO_3)_3 \cdot 6H_2O$ at H//Z direction.

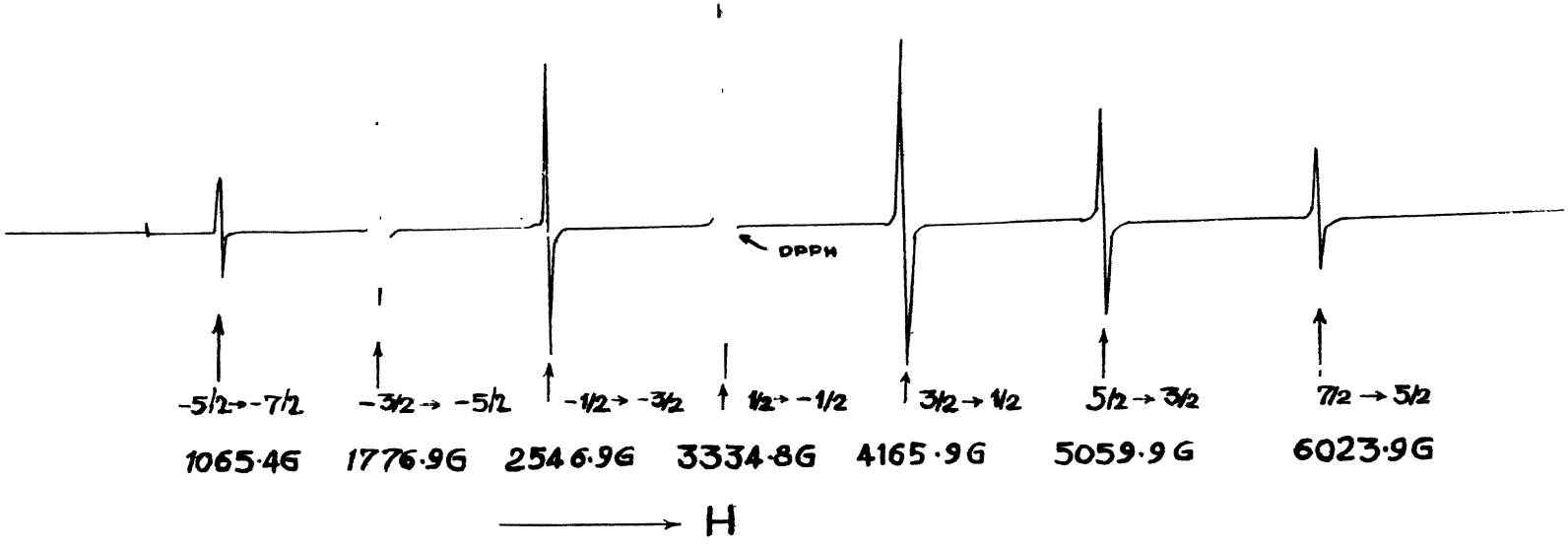
DPPH
-5/2→-7/2
-3/2→-5/2
-1/2→-3/2
1/2→-1/2
3/2→1/2
5/2→3/2
7/2→5/2
1065·4G
1776·9G
2546·9G
3334·8G
4165·9G
5059·9G
6023·9G
H

3+

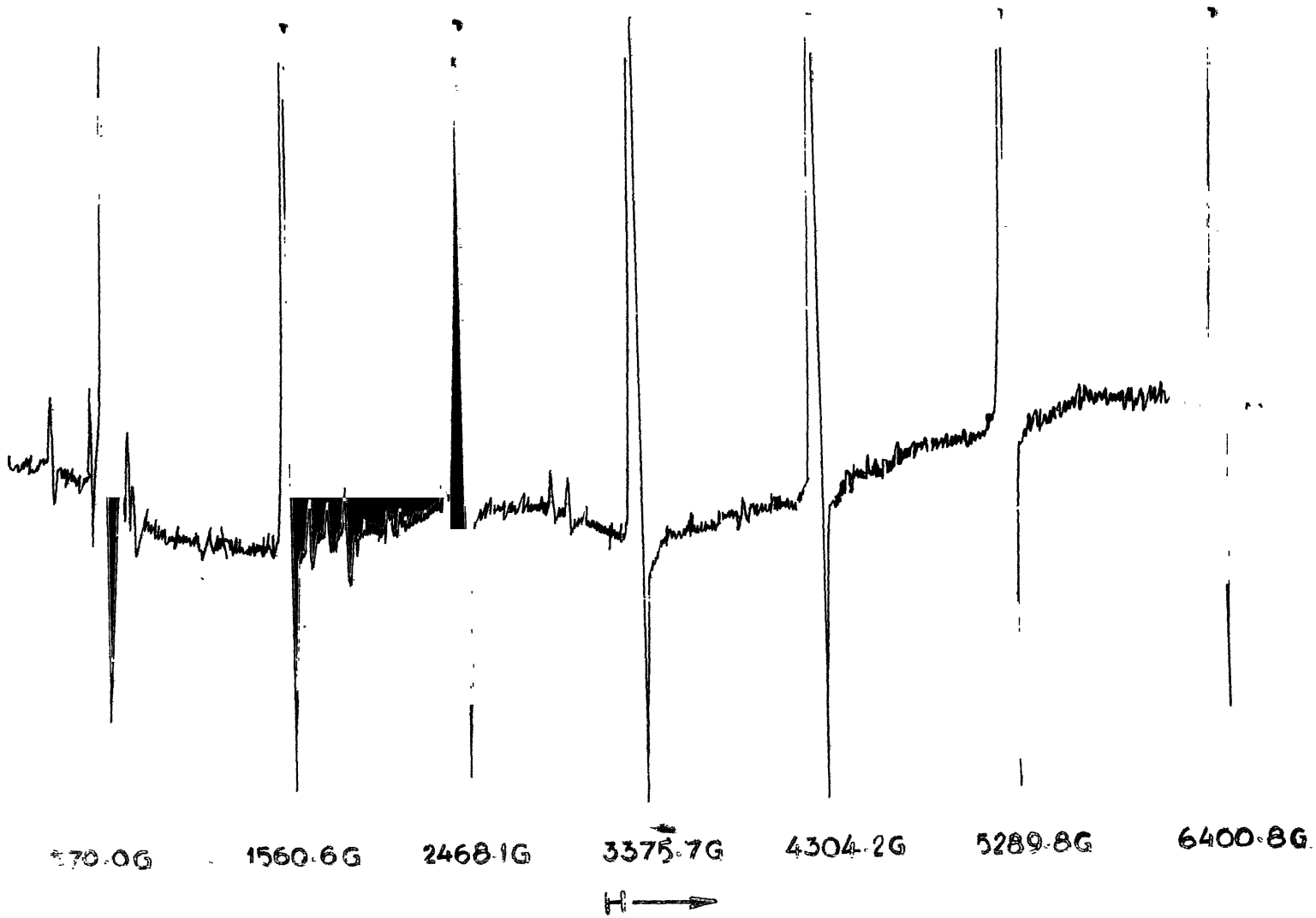
570.0G
1560.6G
2468.1G
3375.7G
4304.2G
5289.8G
6400.8G
H

Table 3.

Observed and Calculated $\Delta M = \pm 1$ transitions of Gd^{3+} doped $Pr(NO_3)_3.6H_2O$ single crystals

Transition	H parallel to the Z-axis		H parallel to the X-axis
	Observed*	Calculated	Observed*
5/2 → 7/2	570.0(G)	563.8(G)	6023.9(G)
3/2 → 5/2	1560.6	1544.3	5059.9
1/2 → 3/2	2468.1	2470.3	4165.9
-1/2 → 1/2	3375.7	3379.8	3334.8
-3/2 → -1/2	4304.2	4305.0	2546.9
-5/2 → -3/2	5289.8	5291.1	1776.9
-7/2 → -5/2	6400.8	6401.0	1065.4
DPPH marker		3385.8(G)	

*Error involved in the observed field values is around ±2 G.

Table 4

Low field transitions of Gd^{3+} doped $Pr(NO_3)_3 . 6H_2O$

Transition	Relative intensity (measured to with in 20%)	Observed**	Expected
$-1/2 \rightarrow -5/2$	5	3026(G)	3036(G)
$3/2 \rightarrow -3/2$	16	728	719 ± 7
$1/2 \rightarrow -5/2$	5	1777	1753
$(-1/2 \rightarrow -7/2)^+$	5	2937	2985
$(5/2 \rightarrow -3/2)^+$	16	350	416 ± 3
$5/2 \rightarrow -5/2$	10	753	748
$3/2 \rightarrow -7/2$	9	1669	1668
$(7/2 \rightarrow -7/2)^+$	24	530	491
Unassigned*	15	1861	

+ The transitions indicated in parentheses show larger deviations between observed and calculated values than other transitions. They are therefore to be taken as doubtful assignments.

* The origin of this line is not well understood. It might be due to some impurity.

** Error involved in the observed field values is around ± 2 G.

References

1. John E. Drumheller, J. Chem. Phys., 38, 870, 1963.

2. W. Low and D. Shaltiel, J. Phys. Chem. Solids, 6, 315,1958.

Chapter V

Paramagnetic Resonance* of Gd^{3+} doped $NdCl_3.6H_2O$, $PrCl_3.7H_2O$ and $Sm(NO_3)_3.6H_2O$ single crystals

Abstract

The paramagnetic resonance spectra of Gd^{3+} doped $NdCl_3.6H_2O$, $PrCl_3.7H_2O$, and $Sm(NO_3)_3.6H_2O$ single crystals have been reinvestigated at room temperature, and the results obtained are discussed in detail. A six line spectrum for H//Z and a seven line spectrum for H//X corresponding to $\Delta M = \pm 1$ transitions, are observed in the case of Gd^{3+} doped $NdCl_3.6H_2O$, where as Gd^{3+} doped $PrCl_3.7H_2O$ and $Sm(NO_3)_3.6H_2O$ show a seven line spectrum for H//Z as well as for H//X. The absence of seventh line in the case of Gd^{3+} doped $NdCl_3.6H_2O$ for H//Z spectrum, is explained as in $SmCl_3.6H_2O$ due to the large Zero-field splitting between $\pm$ 7/2 and $\pm$ 5/2 levels. The angular variation of the observed spectra in ZX plane from $\theta = 0^\circ$ to $\theta = 90^\circ$, is studied in the case of Gd^{3+} doped $NdCl_3.7H_2O$ and $PrCl_3.7H_2O$ single crystals. The spin Hamiltonian analyses are presented. A number of lines have been observed in the low field region in the case of Gd^{3+} doped $PrCl_3.7H_2O$ and they have been analysed as due to transitions with $\Delta M \geqslant 2$.

---

* A part of this is to be published in the J.Chem. Phys.

Introduction

Upreti[1] of this laboratory carried out a study of the electron paramagnetic resonance of Gd^{3+} in single crystals of $NdCl_3.6H_2O$, $PrCl_3.7H_2O$, and $Sm(NO_3)_3.6H_2O$. He took the natural samples in which gadolinium was present as impurity, and grew small single crystals. The planes were not well developed in these crystals and hence the determination of axes was difficult. He did not use the sixth order terms in the spin Hamiltonian and studied only H//Z spectra, due to which it was not possible for him to determine the relative sign of b_2^2 parameter. I have taken up this study in order to improve upon his results. The single crystals with well developed planes are grown in the present experiments by the slow evaporation of the solutions of $NdCl_3.6H_2O$, $PrCl_3.7H_2O$, and $Sm(NO_3)_3.6H_2O$ having a small amount of gadolinium as impurity to which about 0.05 mole percent of the latter has been further added. This resulted in the enhancement of the intensity of the spectra. Apart from the $\Delta M = \pm 1$ transitions observed by Upreti, a number of low field transitions ($\Delta M \geqslant 2$) have been observed here in the case of Gd^{3+} doped $PrCl_3.7H_2O$ single crystals. The present study revealed that the determination of the Z-axes in the earlier work was in error, particularly in the case of Gd^{3+} doped $NdCl_3.6H_2O$ single crystals, the reason being probably that the small crystals used did not show well developed planes. Further in the present work I have taken into account the sixth order terms in the spin Hamiltonian and analysed H//Z as well as H//X spectra and found the relative sign of b_2^2 parameter in all the three crystals studied. The use of the sixth order terms has increased considerably

the agreement between the observed and calculated line positions.

Experimental Results and Discussions

The resonance field equations for $\Delta M = \pm 1$ and $\Delta M \geq 2$ transitions are the same as given in Chapter II. The experimental procedure is the same as described in Chapter III. $NdCl_3.6H_2O$ is a monoclinic crystal[2] with $\beta = 93^\circ$, $a = 9.72\text{A}^\circ$, $b = 6.6\text{A}^\circ$, and $c = 7.9\text{A}^\circ$ where as $PrCl_3.7H_2O$ is a triclinic crystal[2] with $\alpha = 107^\circ$, $\beta = 98^\circ\ 40'$, $\gamma = 72^\circ$, $a = 8.2\text{A}^\circ$, $b = 9.0\text{A}^\circ$, and $c = 8.0\text{A}^\circ$. $Sm(NO_3)_3.6H_2O$ is a triclinic crystal for which no crystallographic data seem to be available.

The Gd^{3+} doped in $NdCl_3.6H_2O$ like that in $SmCl_3.6H_2O$ shows a six line spectrum for H//Z and a seven line spectrum for H//X corresponding to $\Delta M = \pm 1$ transitions, shown in figs. 7, and 8, respectively. The peak to peak derivative width of lines is about 20-25 gauss. The angular variation in the ZX plane from $\theta = 0^\circ$ to $\theta = 90^\circ$ is shown in fig. 9. The Zero-field splittings are such that while one observes seven lines for H//X, only six lines are observed for H//Z. All the seven lines can be followed from $\theta = 90^\circ$ to $\theta = 47^\circ$, the seventh line being unobservable for $\theta < 47^\circ$ where θ is the angle between H and Z-axis. The absorption lines other than $\Delta M = \pm 1$ transitions.for H//Z and H//X probably correspond to the low field transitions ($\Delta M \geq 2$).

The Gd^{3+} doped $PrCl_3.7H_2O$ shows a seven line spectrum for H//Z as well as for H//X corresponding to $\Delta M = \pm 1$ transitions, shown in figs. 10, and 11, respectively. The peak to peak derivative width of

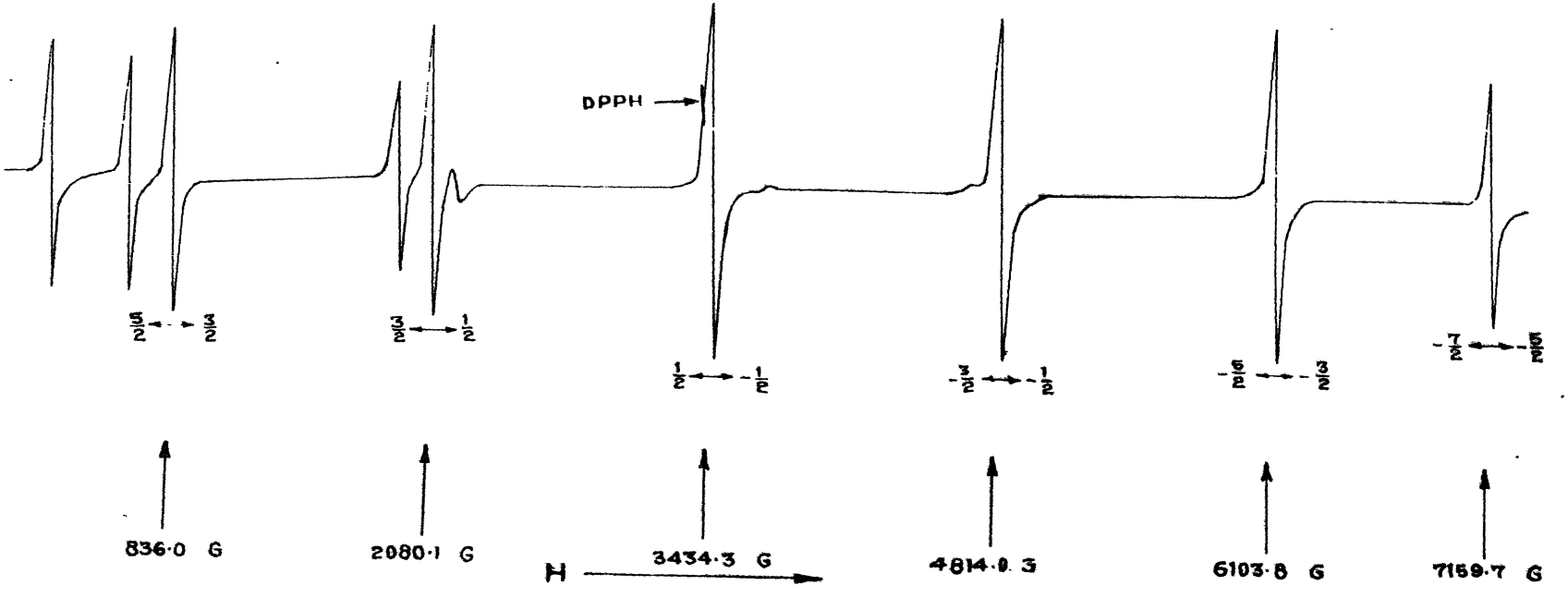

Fig.7. EPR spectrum of Gd^{3+} in single crystals of $NdCl_3.6H_2O$ at H//Z direction

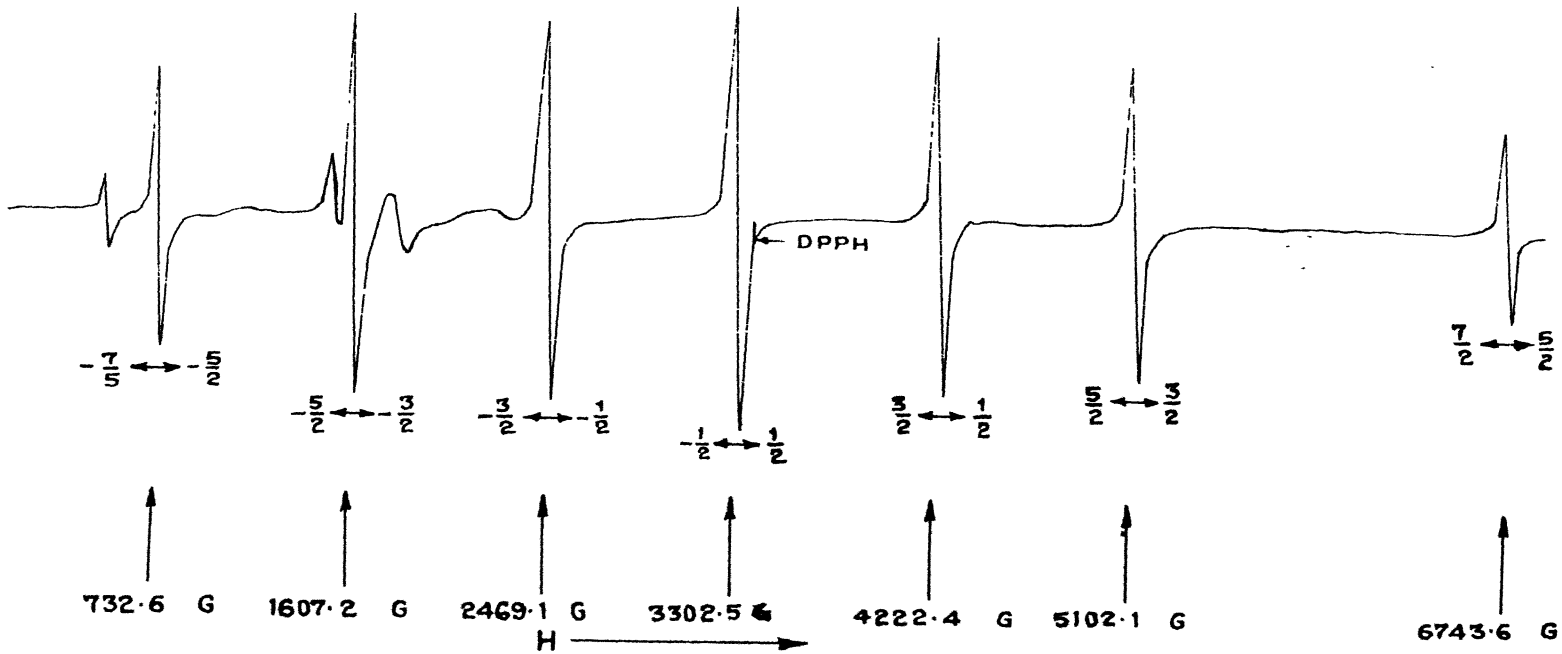

Fig. 8. EPR spectrum of Gd^{3+} in single crystals of $NdCl_3 . 6H_2O$ at H//X direction

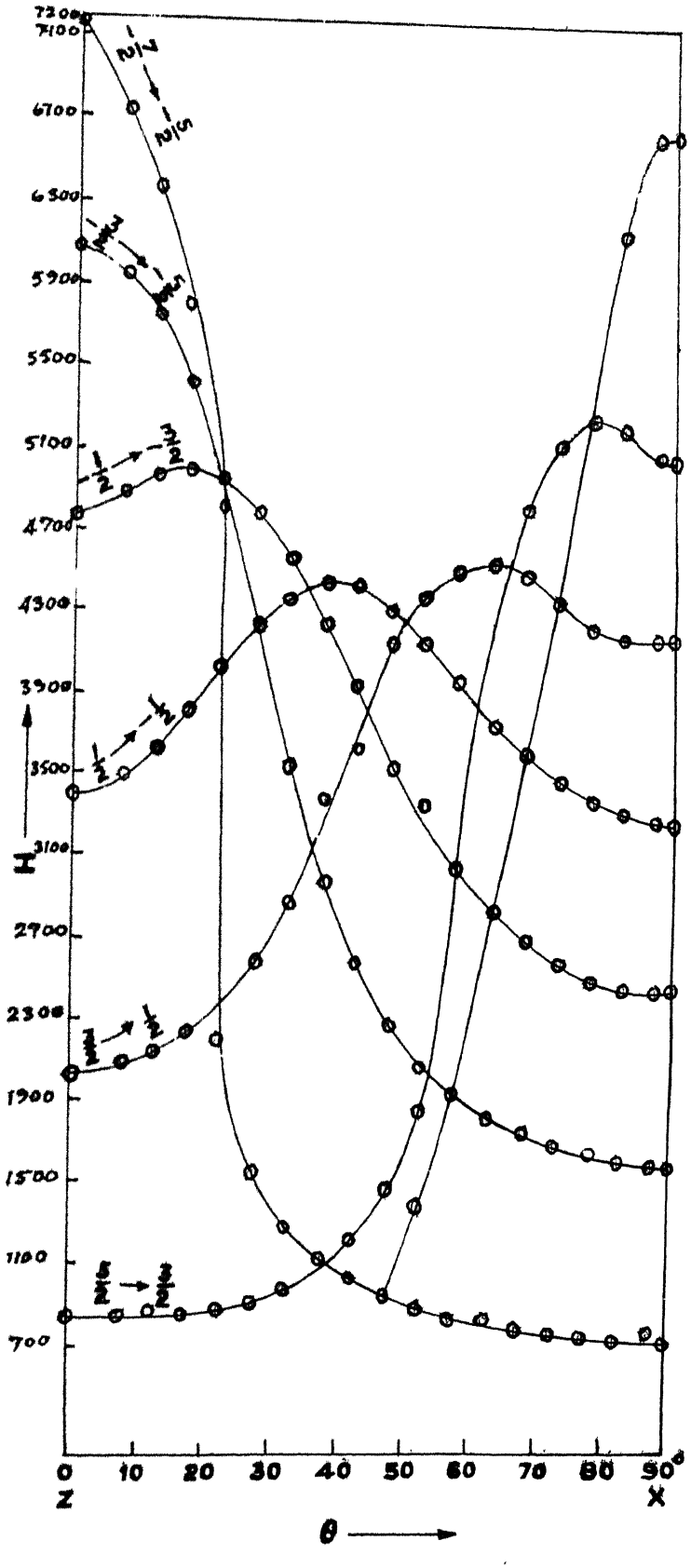

Fig. 9. Angular Variation of the EPR of Gd^{3+} in single crystals of $NdCl_3 . 6H_2O$

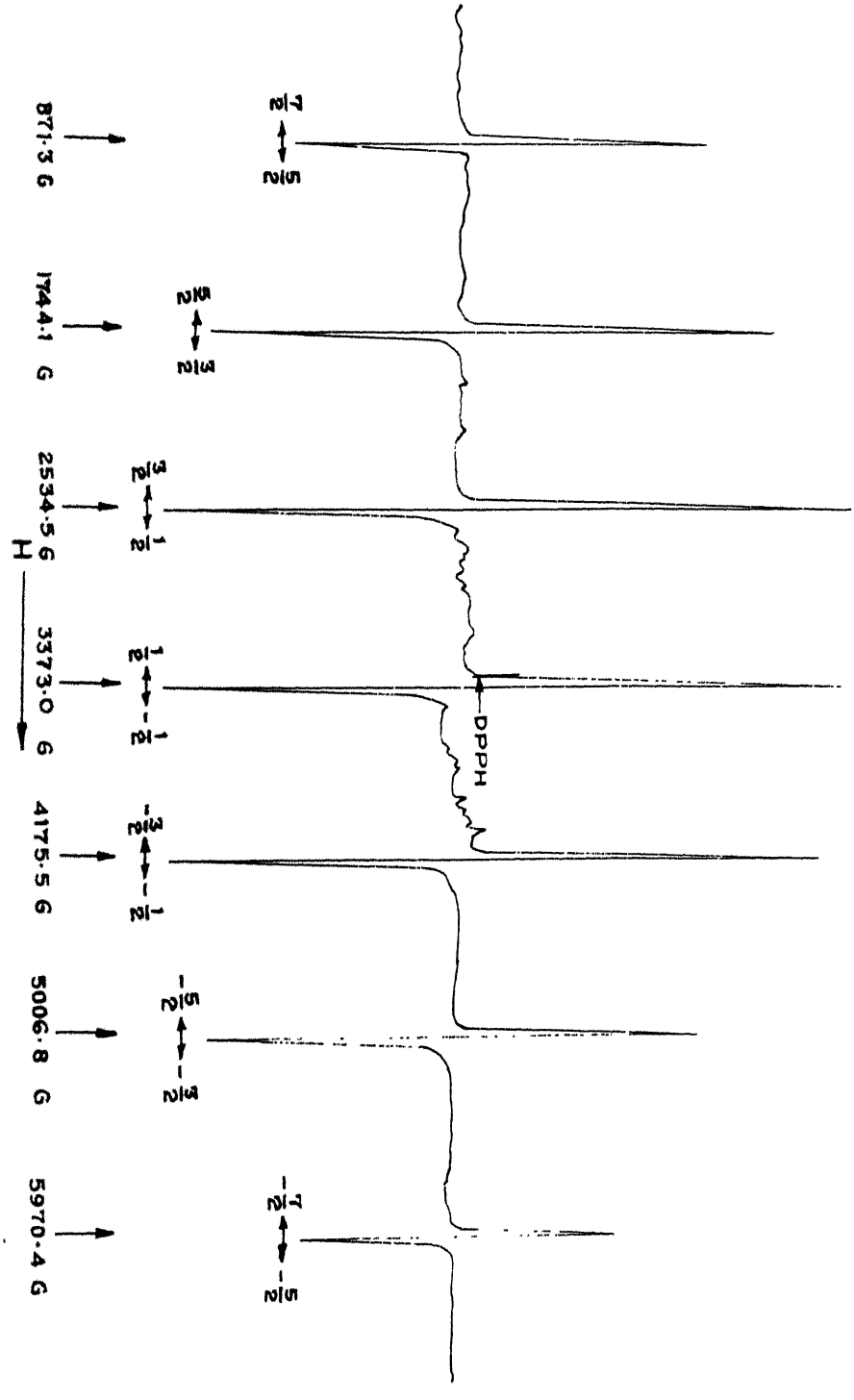

Fig. 10. ESR spectrum of Gd^{3+} in single crystals of $LaCl_3 \cdot 7H_2O$ at X/a direction.

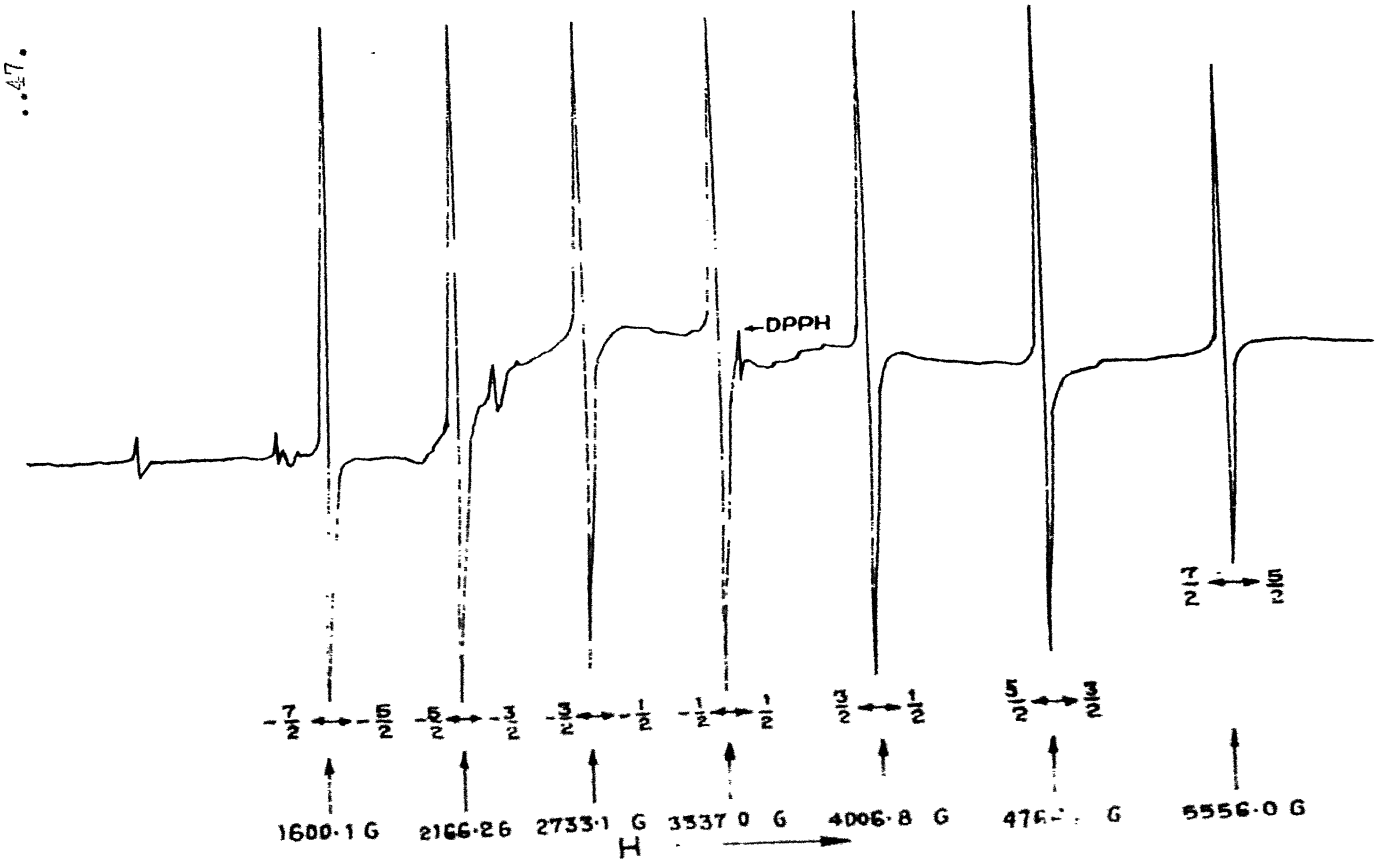

Fig. 12. EPR spectrum of Gd^{3+} in single crystals of $PrCl_3.7H_2O$ at H//X direction.

the observed absorption lines is about 15-19 gauss. Their angular variation in ZX plane from $\theta = 0^{\circ}$ to $\theta = 90^{\circ}$ is shown in fig. 12. Apart from the $\Delta M = \pm 1$ transitions a number of low field transitions have also been observed. These varied in position and intensity as the magnetic field is rotated with respect to the z-axis. A careful study of these lines is made for H//Z direction and the observed transitions are shown in Fig. 13, along with $\Delta M = \pm 1$ transitions.

The Gd^{3+} doped $Sm(NO_3)_3.6H_2O$ also shows a seven line spectrum for H//Z as well as for H//X corresponding to $\Delta M = \pm 1$, shown in figs. 14 and 15, respectively. The peak to peak derivative width of the absorption lines is about 11-14 gauss.

The parameters of the spin Hamiltonian are obtained in the manner described in Chapter II and are listed in table 5 in the case of Gd^{3+} doped $NdCl_3.6H_2O$, $PrCl_3\ 7H_2O$, and $Sm(NO_3)_3.6H_2O$ single crystals. The resonance fields corresponding to $\Delta M = \pm 1$ transitions for H//Z are calculated using the parameters listed in table 5 and are given in table 6 along with the observed resonance fields.

The relative separations between the four doublets corresponding to the Zero-field energy levels have been calculated for Gd^{3+} ion in the three crystals studied and are given in table 7.

An attempt is made to identify the low field transitions in the case of Gd^{3+} $PrCl_3.7H_2O$ by comparing the observed transitions with the theoretically expected positions. The resonance fields correspondir to these lines are listed in table 8 along with the assigned

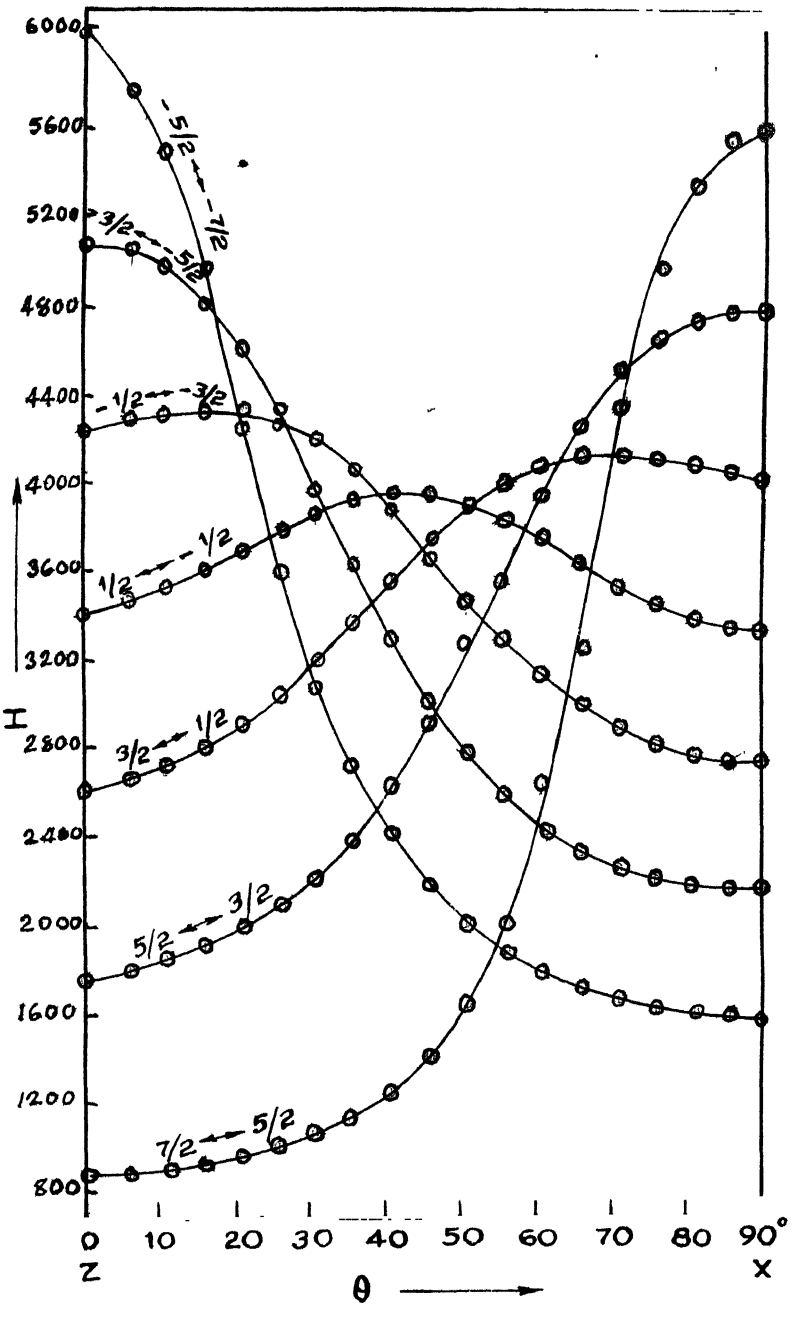

Fig. 12. Angular variation of the EPR of Gd^{3+} in single crystals of $PrCl_3.7H_2O$

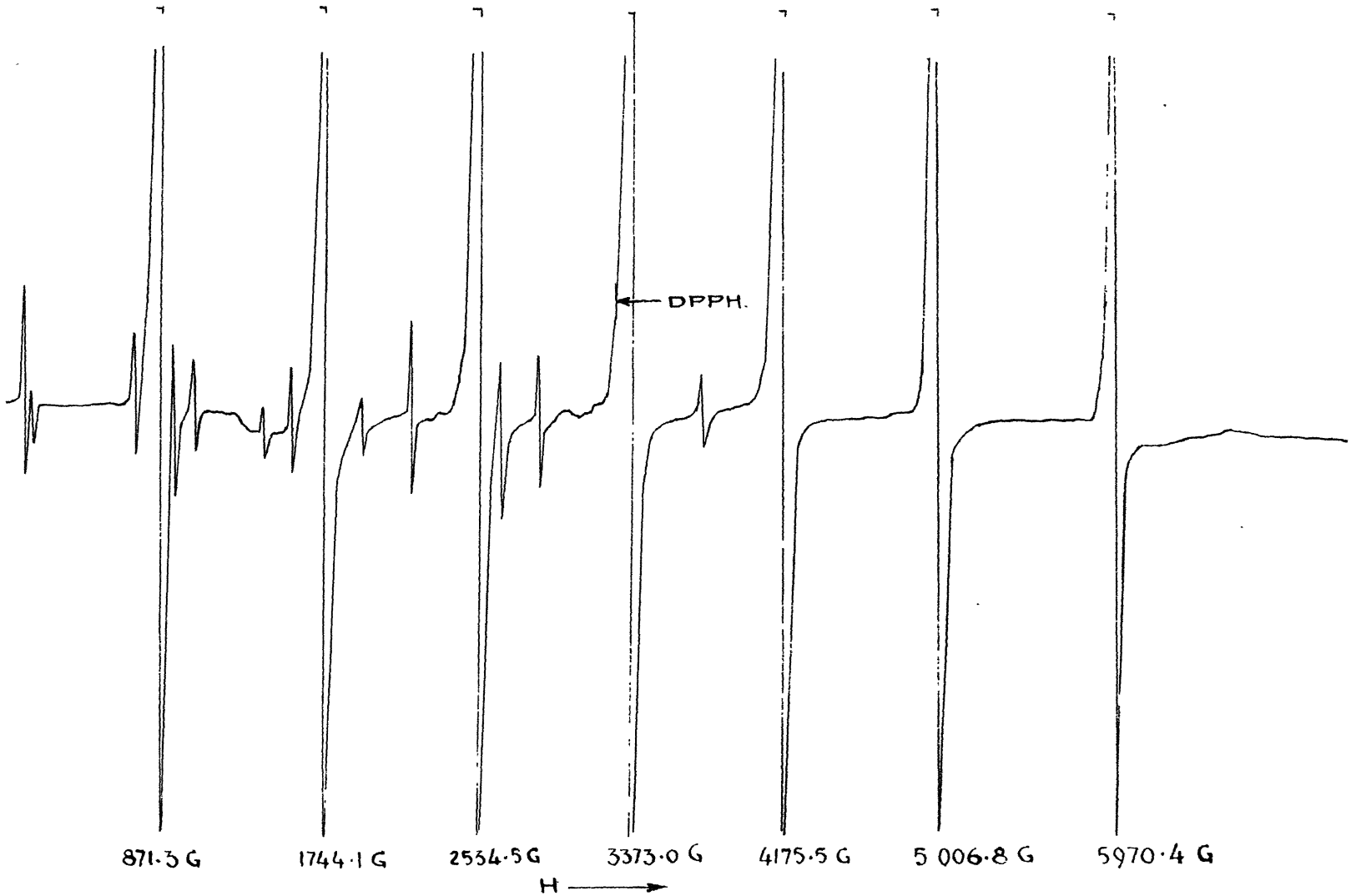

Fig. 13. Low field transitions of Gd^{3+} in single crystals of $PrCl_3.7H_2O$ along with seven

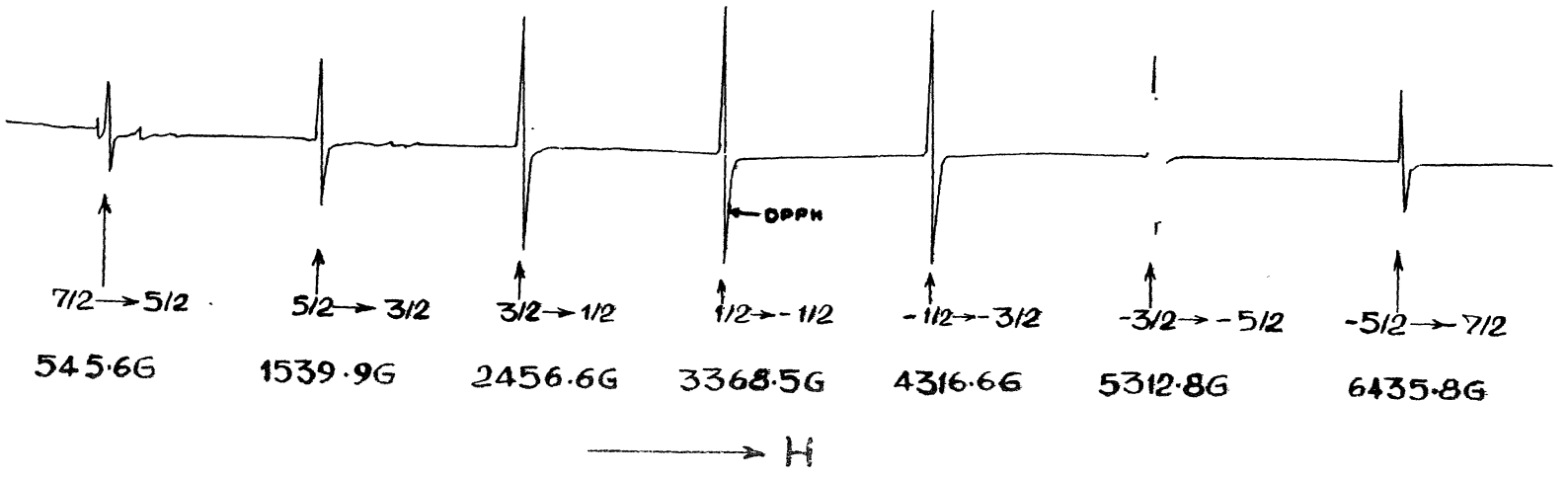

Fig. 14. EPR spectrum of Gd^{3+} in single crystals of $Sm(NO_3)_3 \cdot 6H_2O$ at H//Z direction.

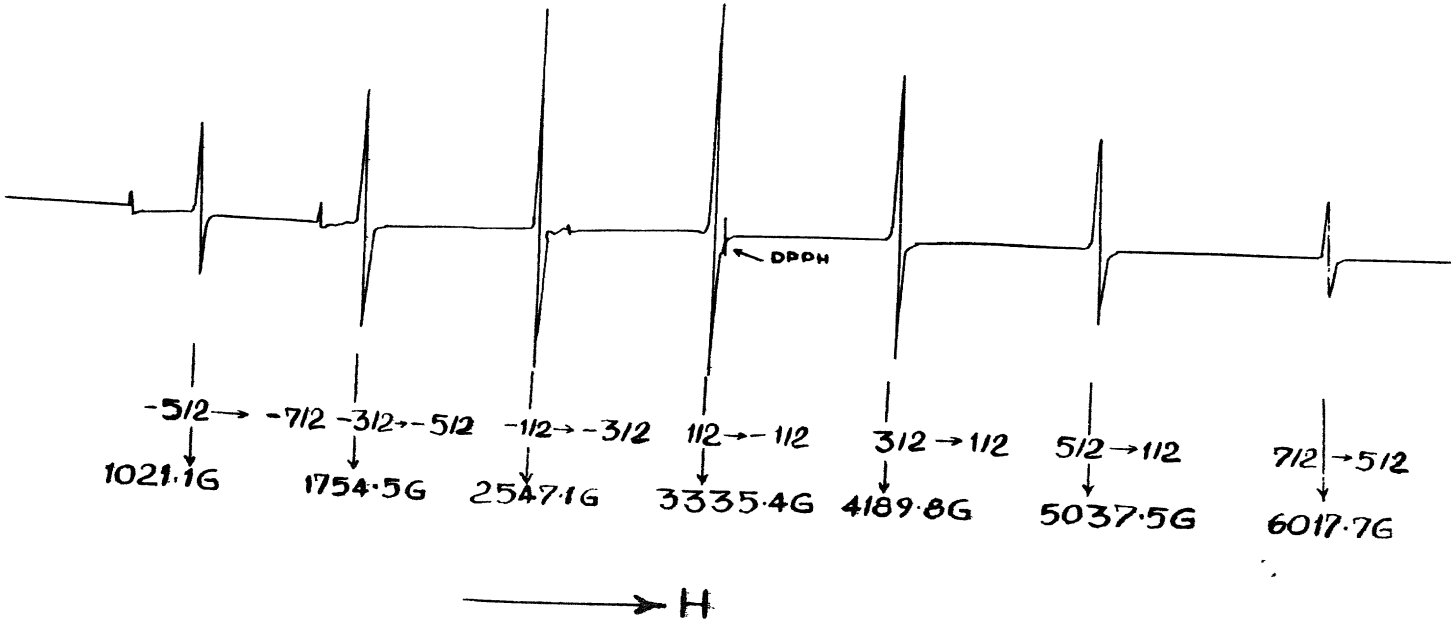

Fig. 15. EPR spectrum of Gd^{3+} in single crystals of $Sm(No_3)_3 . 6H_2O$ at H//X direction.

Table 5

The spin Hamiltonian parameters of Gd^{3+} doped $NdCl_3.6H_2O$, $PrCl_3.7H_2O$, and $Sm(NO_3)_3.6H_2O$ single crystals

	Gd^{3+} doped $NdCl_3.6H_2O$	Gd^{3+} doped $PrCl_3.7H_2O$	Gd^{3+} doped $Sm(NO_3)_3.6H_2O$
$g_{\parallel}$	1.987 ± .002	1.976 ± .002	1.996 ± .002
$g_{\perp}$	1.986 ± .002	1.960 ± .002	1.987 ± .002
b_2^o	659.77 (G)	419.60 (G)	494.60 (G)
b_4^o	-11.86	2.33	1.40
b_6^o	-0.45	.74	0.14
b_2^2	-414.23	-263.40	-388.0
$b_4^4-b_4^2$	48.86	7.73	10.2
$b_6^6-b_6^4+b_6^2$	-8.65	-15.0	8.7

transitions and theoretically expected resonance fields.

The assignments for low field transitions in the case of Gd^{3+} doped $PrCl_3.7H_2O$ single crystals are to be taken as tentative for the same reason mentioned in the case of Gd^{3+} $Pr(NO_3)_3.6H_2O$ single crystals in Chapter IV.

Table 6

Observed and calculated $\Delta M = \pm 1$ transitions of Gd^{3+} doped $NdCl_3.6H_2O$, $PrCl_3.7H_2O$ and $Sm(NO_3)_3.6H_2O$ single crystals

Transition	Gd^{3+} doped $NdCl_3.6H_2O$		Gd^{3+} doped $PrCl_3.7H_2O$		Gd^{3+} doped $Sm(NO_3)_3.6H_2O$	
	Observed*	Calculated	Observed*	Calculated	Observed*	Calculated
7/2 → 5/2	unobservable		871.3 (G)	871.3 (G)	545.6 (G)	539.3 (G)
5/2 → 3/2	836.0 (G)	827.9 (G)	1744.1	1762.3	1539.9	1525.0
3/2 → 1/2	2090.1	2079.8	2564.5	2566.5	2456.6	2459.6
1/2 → -1/2	3434.3	3438.4	3373.0	3366.0	3368.5	3380.5
-3/2 → -1/2	4814.0	4813.6	4175.5	4175.5	4316.6	4317.8
-5/2 → -3/2	6103.8	6103.7	5006.8	5006.9	5312.8	5314.5
-7/2 → -5/2	7159.7	7159.8	5970.4	5970.4	6435.8	6436.1
DPPH marker	3380.1(G)		3352.6(G)		3383.7(G)	

* Error involved in the observed field values is around ±2 G.

Table 7

Relative separations between the Zero-field energy levels of Gd^{3+} in $NdCl_3.6H_2O$, $PrCl_3.7H_2O$, and $Sm(NO_3)_3.6H_2O$ single crystals

	Gd^{3+} doped $NdCl_3.6H_2O$	Gd^{3+} doped $PrCl_3.7H_2O$	Gd^{3+}doped $Sm(NO_3)_3$
$\pm 7/2 \leftrightarrow \pm 5/2$	9.94 kmc	6.82 kmc	7.82 kmc
$\pm 5/2 \leftrightarrow \pm 3/2$	7.06	4.15	5.0
$\pm 3/2 \leftrightarrow \pm 1/2$	7.26	4.43	6.18

For H//Z, the relative separation between $\pm$ 7/2 and $\pm$ 5/2 levels in the case of Gd^{3+} doped $NdCl_3.6H_2O$ is found to be larger than the maximum frequency of the spectrometer used and this observation explains clearly the absence of the + 7/2 $\leftrightarrow$ + 5/2 transition in the present experiments. As pointed out in Chapter III for Gd^{3+} doped in $SmCl_3.6H_2O$, one may expect to observe this transition and therefore all the seven lines of Gd^{3+} inn by doing the EPR work in the K-band region or other higher frequency regions.

Table 8

Low field transitions of Gd^{3+} in $PrCl_3.7H_2O$

Transition	Relative intensity (measured to within 20%)	Observed**	Calculated
-1/2 → -5/2	32	2906 (G)	2872 (G)
-3/2 → -7/2	12	3787	3789
3/2 → -3/2	28	971	901
1/2 → -5/2	5	1795	1807
-1/2 → -7/2	24	2707	2768
1/2 → -7/2	28	2234	2187±14.5
5/2 → -5/2	23	758	721
3/2 → -7/2	20	1585	1527
7/2 → -5/2	19	171	157
5/2 → -7/2	19	1059	992
Unassigned*	11	212	
Unassigned*	10	1433	
Unassigned*	9	1944	

* The origin of these lines is not well understood. They might be due to some impurities.

** Error involved in the observed field values is around ±2G.

References

1. G.C. Uproti - Ph.D. thesis (1966) submitted to the Indian Institute of Technology, Kanpur, India.

2. ACA monograph number 5 - crystal data determinative tables (2nd addition) Donnay and Donnay.

Chapter VI

Paramagnetic Resonance of Gd^{3+} doped $La(NO_3)_3.6H_2O$ and $Nd(NO_3)_3.6H_2O$ single crystals

Abstract

The paramagnetic resonance of Gd^{3+} in single crystals of $La(NO_3)_3.6H_2O$ and $Nd(NO_3).6H_2O$ are studied. A seven line spectrum for H//Z as well as for H//X corresponding to $\Delta M = \pm 1$ transitions, are observed in these crystals. The spin Hamiltonian analyses are presented. The estimated Zero-field splittings of Gd^{3+} in the various single crystals studied in the thesis are compared with one another and discussed. The reasons for the absence of detectable hyperfine structure in the present experiments are indicated.

Introduction

A paramagnetic resonance study of $Gd(NO_3)_3.6H_2O$ was carried out by Garif'yanov[1] where he took single crystals of $Gd(NO_3)_3.6H_2O$ diluted with ten parts of $La(NO_3)_3.6H_2O$ and reported a spectrum corresponding to cubic crystalline field at gadolinium site with $a = .176$ cm^{-1}. It was felt that it would be interesting to study the paramagnetic resonance of Gd^{3+} doped $La(NO_3)_3.6H_2O$ single crystals. Therefore single crystals are grown from the solution of $La(NO_3)_3.6H_2O$ having a small amount of gadolinium as impurity to which about 0.05 mole percent of the latter has been further added. The spectra corresponding to site symmetry much lower than cubic are observed and analysed using the spin Hamiltonian given in Chapter III.

The present Chapter also deals with the paramagnetic resonance of Gd^{3+} doped $Nd(NO_3)_3.6H_2O$ single crystals, grown by the same method as used in the case of Gd^{3+} doped $La(NO_3)_3.6H_2O$. The observed spectra are analysed by using the same spin Hamiltonian.

Experimental Results and Discussions

The experimental procedure is the same as given in Chapter III. $La(NO_3)_3.6H_2O$ and $Nd(NO_3)_3.6H_2O$ are triclinic crystals for which no crystallographic structures seem to be available. The EPR of Gd^{3+} doped in these crystals shows a seven line spectrum for H//Z as well as for H//X corresponding to the $\Delta M = \pm 1$ transitions. The observed spectra are shown in figs. 16,17,18, and 19, respectively. The peak to peak derivative width of the observed absorption lines is about 30-40

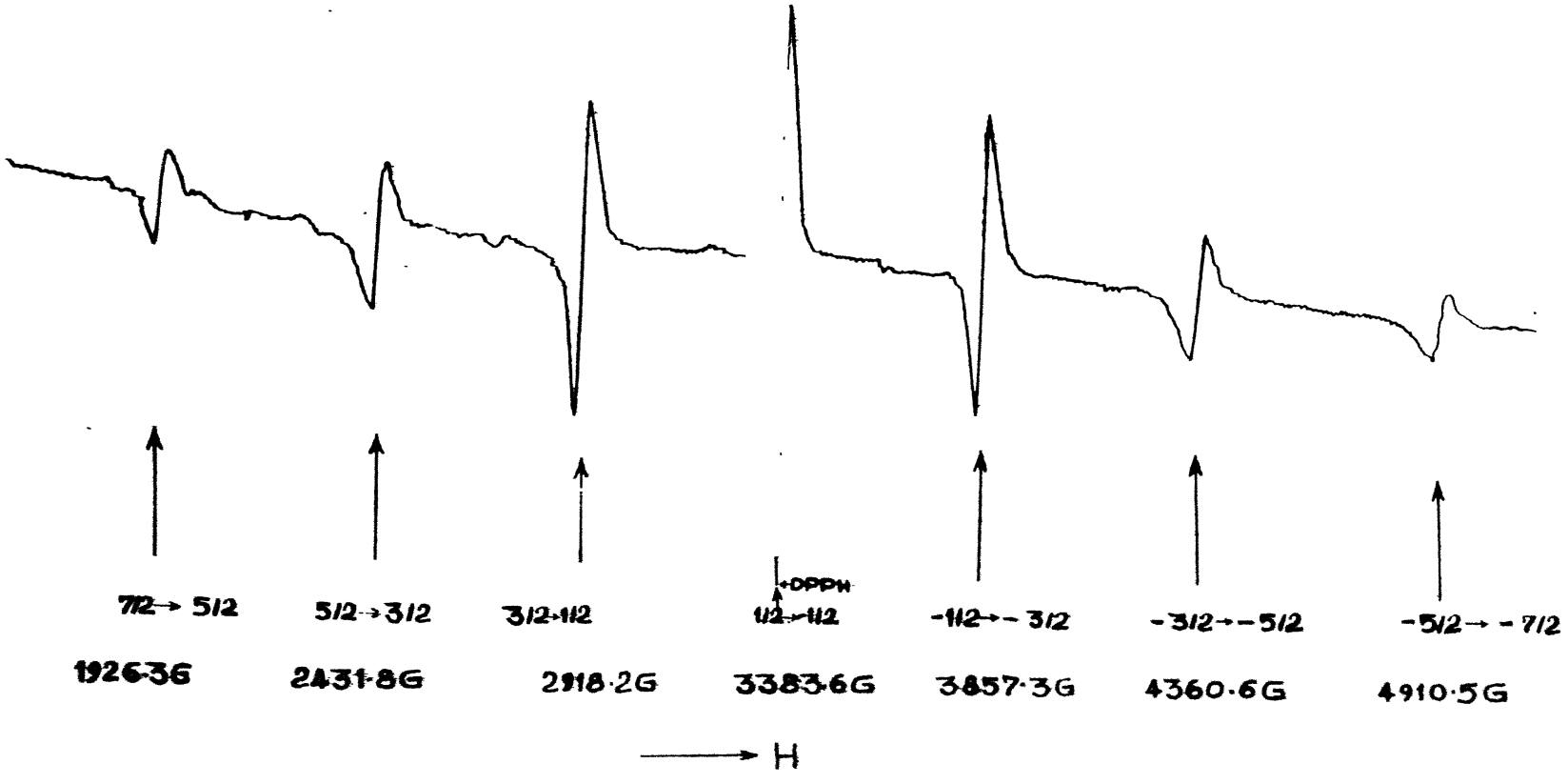

Fig.16. EPR spectrum of Gd^{3+} in single crystals of $La(NO_3)_3.6H_2O$ at H//c direction

Fig.17. EPR spectrum of Gd^{3+} in single crystals of $La(NO_3)_3.6H_2O$ at H//X direction

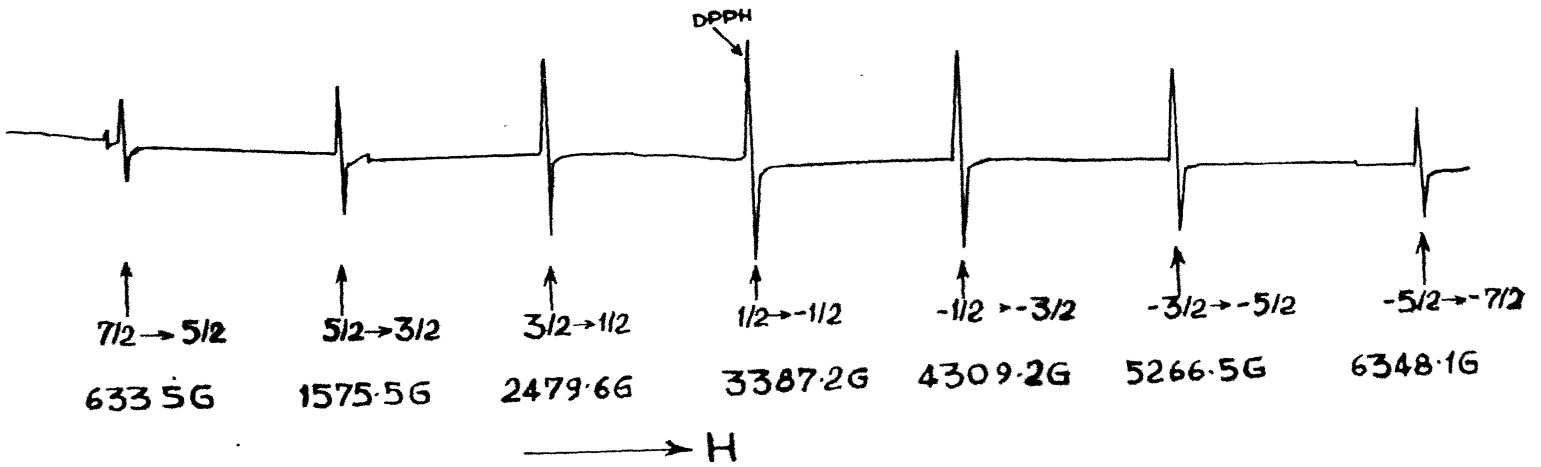

Fig.18. EPR pectrum of Gd^{3+} in single crystals of $Nd(NO_3)_3.6H_2O$ at H//Z direction

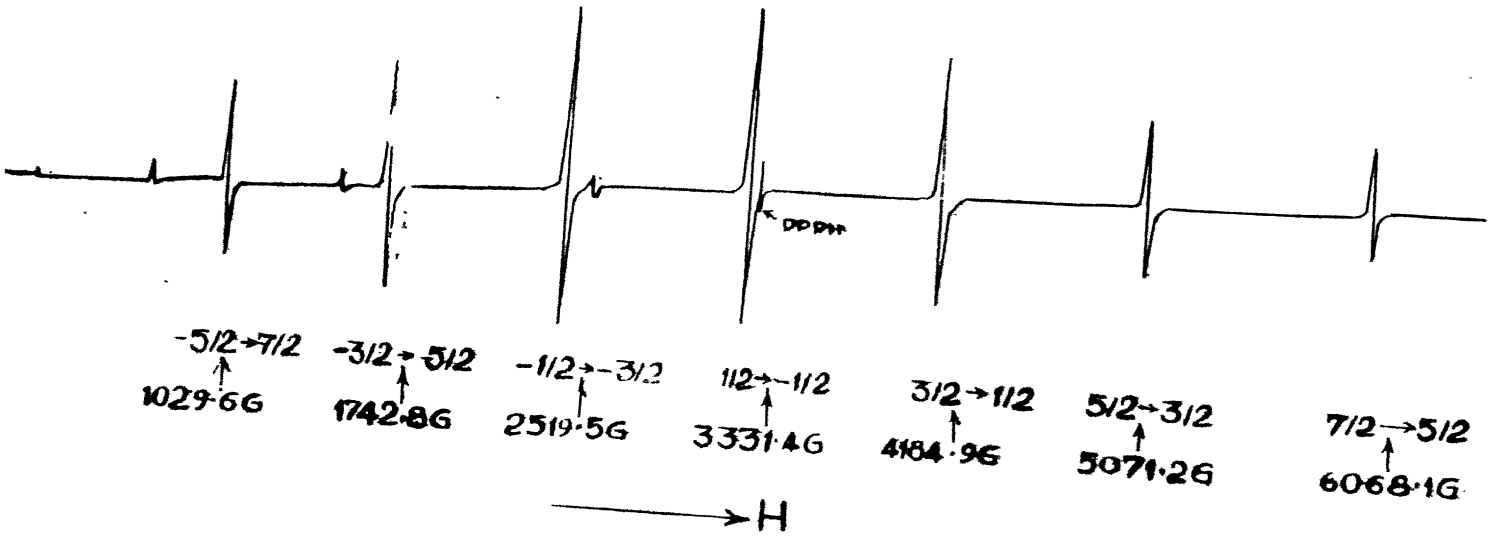

Fig.19. EPR spectrum of Gd^{3+} in single crystals of $Nd(NO_3)_3.6H_2O$ at H//X direction

gauss in the case of Gd^{3+} doped $Nd(NO_3)_3.6H_2O$ single crystal. The angular variation of the observed $\Delta M = \pm 1$ transitions in the case of Gd^{3+} doped $La(NO_3)_3.6H_2O$ single crystals is studied in the ZX pl from $\theta = 0^\circ$ to $\theta = 90^\circ$ as shown in fig. 20. The additional weak lines other than $\Delta M = \pm 1$ transitions in the case of Gd^{3+} doped $Nd(NO_3)_3.6H_2O$ single crystals might be corresponding to the low fie transitions ($\Delta M \geqslant 2$).

The parameters of the spin Hamiltonian are obtained in the manner described in Chapter II and are listed in table 9.

Table 9

The spin Hamiltonian parameters of Gd^{3+} doped $La(NO_3)_3.6H_2O$ and $Nd(NO_3)_3 . 6H_2O$ single crystals

	Gd^{3+} doped $La(NO_3)_3.6H_2O$	Gd^{3+} doped $Nd(NO_3)_3.6H_2O$
$g_{\|\|}$	1.995 ± .002	1.984 ± .002
$g_\perp$	1.986 ± .002	1.992 ± .002
b_2^0	246.6 (G)	480.0 (G)
b_4^0	0.93	0.73
b_6^0	0.1	0.54
b_2^2	-222.4	-392.0
$b_4^4-b_4^2$	6.49	18.93
$b_6^6-b_6^4+b_6^2$	-3.34	3.98

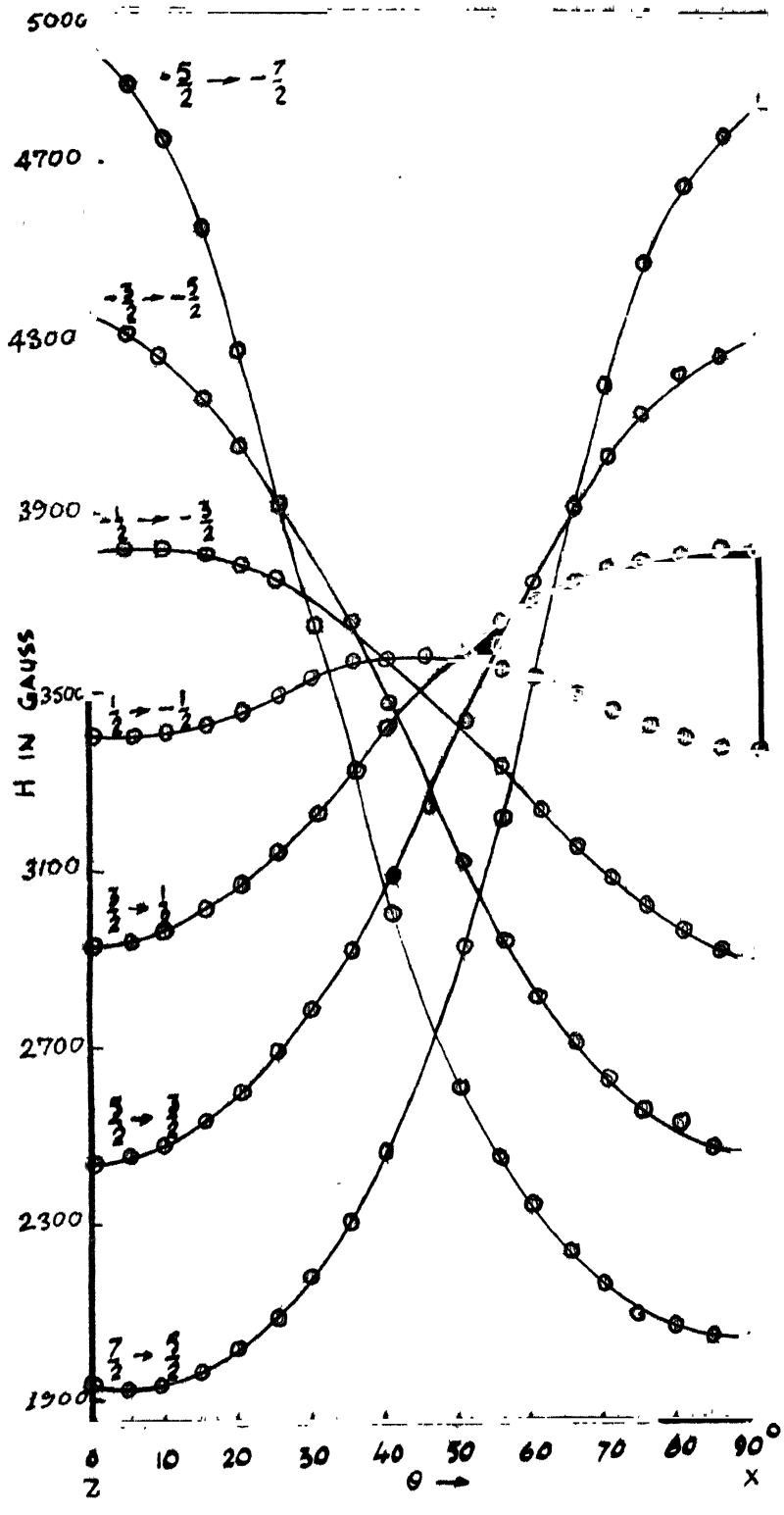

Fig.20. Angular variation of the EPR of Gd^{3+} in single crystals of $La(NO_3)_3.6H_2O$

The resonance fields corresponding to $\Delta M = \pm 1$ transitions for H//Z are calculated using the parameters listed in table 9, and are given in table 10, along with the observed resonance fields for H//Z in both the crystals.

The calculated relative separations between the four doublets corresponding to zero-field energy levels are given in table 11 in the case of Gd^{3+} doped $La(NO_3)_3.6H_2O$ and $Nd(NO_3)_3.6H_2O$ single crystals. Where in the corresponding values obtained in the other crystals studied in the thesis are also included for comparison. The values of b_2^0 obtained for the various crystals are listed in the table 12 for convenient reference.

It is interesting to see that the b_2^0 values and zero-field splittings of Gd^{3+} in the chlorides of Nd and Sm are greater than those in the corresponding nitrates. This type of comparison may not have much meaning in the case of the praseodymium salts studied here as the water of crystallization is not the same in both. The b_2^0 values and the total spreads of zero-field splittings of Gd^{3+} ion in the nitrates of Pr, Nd, and Sm are practically same, the average total splitting spread being 18.7 kmc. The splitting in these salts is much larger (practically twice) than that in lanthanum nitrate, which indicates that the unfilled electrons of the f shells of the host lattice play an important role in the zero-field splittings of the energy levels of impurity ion. The fact that zero-field splittings of Gd^{3+} ion in the nitrates of Pr, Nd, and Sm are approximately same implies that the zero-field splittings in the case of the chlorides of Pr, Nd, and Sm might also be same. This is found to be true for the

Table 10

Observed and Calculated $\Delta M = \pm 1$ transitions of Gd^{3+} doped $La(NO_3)_3.6H_2O$ and $Nd(NO_3)_3.6H_2O$ single crystals for H//Z

Transition	Gd^{3+} doped $La(NO_3)_3.6H_2O$		Gd^{3+} doped $Nd(NO_3)_3.6H_2O$	
	Observed*	Calculated	Observed*	Calculated
5/2 → 7/2	1926.3 (G)	1926.7 (G)	633.5 (G)	644.6 (G)
3/2 → 5/2	2431.8	2428.5	1575.5	1587.8
1/2 → 3/2	2918.2	2903.7	2479.6	2480.1
-1/2 → 1/2	3383.5	3376.2	3387.2	3385.4
-3/2 → -1/2	3857.3	3857.7	4309.2	4309.1
-5/2 → -3/2	4360.6	4360.6	5266.5	5266.3
-7/2 → -5/2	4910.5	4910.2	6348.1	6347.8
DPPH marker	3383.5(G)		3383.8(G)	

*Error involved in the observed field values is around ±2G.

chlorides of Nd and Sm studied here but not for the chloride of Pr. This deviation in the case of $PrCl_3.7H_2O$ may probably be because of its water of crystallization being different from that of the other two chlorides studied. The water of crystallization apparently plays its role in the development of the crystal field strengths and therefore also in zero-field splittings.

The presence of the only one set of spectrum corresponding to $\Delta M = \pm 1$ transitions in all the crystals studied in the thesis, shows that gadolinium ion occupies only one observable type of rare earth site in these crystals.

Table 11

Relative separations between the zero-field energy levels of Gd^{3+} in crystals

	$La(NO_3)_3.6H_2O$	$Pr(NO_3)_3.6H_2O$	$Nd(NO_3)_3.6H_2O$	$Sm(NO_3)_3.6H_2O$	$NdCl_3.6H_2O$	$SmCl_3.6H_2O$	$PrCl_3.7H_2O$
$\pm 7/2 \leftrightarrow \pm 5/2$	3.82 kmc	7.74 kmc	7.48 kmc	7.82 kmc	9.94 kmc	10 kmc	6.82 kmc
$\pm 5/2 \leftrightarrow \pm 3/2$	2.52	4.93	4.84	5.0	7.06	7.1	4.15
$\pm 3/2 \leftrightarrow \pm 1/2$	3.41	6.01	6.16	6.18	7.26	7.4	4.43
Total spread of the splitting	9.75	18.68	18.48	19.0	24.26	24.5	15.4

Table 12

The values of b_2^0 parameter in gauss for Gd^{3+} in crystals

$La(NO_3)_3.6H_2O$	$Pr(NO_3)_3.6H_2O$	$Nd(NO_3)_3.6H_2O$	$Sm(NO_3)_3.6H_2O$	$NdCl_3.6H_2O$	$SmCl_3.6H_2O$	$PrCl_3.7H_2O$
246.6	488.5	480.0	494.6	659.77	667.7	419.6

There are two isotopes of Gd^{3+} (155,157) that have a nuclear spin 3/2 with relative abundance 14.7 and 15.7%, respectively. The $Gd^{156,158,160}$ and others which total about 70% will have no hyperfine interaction while Gd^{155} and Gd^{157} will have. The absence of the hyperfine structure in the present experiments (Chapter III to VI) could be explained probably due to the large width of observed absorption lines. It may be noted that the hyperfine structure reported so far for Gd^{3+} ion is either in the cases where the absorption lines are sufficiently narrow[2,3] for the hyperfine structure to be clearly visible or in the case of samples enriched[4] with $Gd^{155,157}$.

References

1. N.S. Garif'yanov, Dokl. Akad. Nauk SSSR, 84, No.5, 923, 1952.

2. (a) D.R. Hutton and G.J. Troup, Brit J. Appl. Phys. 15, 405,1964.

(b) C.F. Hempstead and K.D. Bowers, Bell Telephone System, Technical publications, monograph 3599.

(c) M.M. Abragam, E.J. Lee, and R.A. Weeks, J. Phys. Chem. Solids, 26, 1249, 1965.

3. W.Low and D. Shaltiel, J. Phys. Chem. Solids, 6, 315, 1958.

4. W. Low, Phys. Rev. 103, 1305, 1956.

Title Of Thesis	Electron Paramagnetic Resonance Of Gd^{3+} in Single Crystals Of Some Hydrated Rare-Earth Nitrates And Chlorides
Full Name	Gur Bachan Singh Chaddha
Place And Date of Birth	Haldwani, (Nainital), 11 February 1943
Earlier Academic Back Ground	Allahabad University, B.Sc., 1962 Allahabad University, M.Sc., 1964
Present Position	A Junior Research Fellow Of The Council Of Scientific And Industrial Research, India Joined as a Ph.D. Student in the Department of Physics, Indian Institute of Technology, Kanpur in July 1964
Department	Physics

Date 30.12.66

Signed GVBSingh